Natural Climate Drivers Dominate in the Current Warming

Antero Ollila

School of Engineering (Emer.)
Aalto University, Espoo, Finland

OPEN ACCESS

Klimarealistene
P.O. Box 33
3199 Porsgrunn
Norway
ISSN: 2703-9072
Correspondence to aveollila@ya-hoo.com
Vol. 3.3 (2023)
pp. 290-326

Abstract

Anthropogenic global warming (AGW) is the prevailing theory of the IPCC for global warming, in which Greenhouse gases (GHGs) are the major drivers, whereas albedo, aerosols, and clouds have had cooling effects, and natural drivers have an insignificant role (<0.8 %). According to Assessment Report 6 (AR6), these radiative forcings (RF) have been a total of 2.70 Wm^{-2} causing a temperature increase of 1.27 °C in 2019. Many research studies are showing significantly lower RF and climate sensitivity values for anthropogenic climate drivers. Research studies offering natural climate drivers as the partial or total solution for global warming have gradually emerged like solar radiation changes, cosmic forces, and multidecadal, century- and millennial-scale climate oscillations. The cloud effects are still a major concern in General Circulation Models (GCMs). The cloudiness changes have a major role in cosmic effects like magnifying the warming effect of the Total Solar Irradiation (TSI). The 60- & 88- year oscillations are the best-known oscillations, which are commonly known as AMO (Atlantic Multidecadal Oscillation) and the Gleissberg cycle explaining the ups and downs of the global temperature in the 1900s. Mechanisms of long-term climate oscillations are still under debate. There are also essential differences between carbon cycle models and GH effect magnitude specifications. The synthesis of these natural climate drivers together with anthropogenic drivers constitutes an alternative theory called Natural Anthropogenic Global Warming (NAGW), in which natural drivers have a major role in dominating the warming during the current warm period. These results mean that there is no climate crisis and a need for prompt CO_2 reduction programs.

Keywords: Anthropogenic climate drivers; natural climate drivers; climate sensitivity; radiative forcing; greenhouse effect; positive water feedback; climate oscillations; carbon circulation; SW radiation anomaly

Submitted 2023-02-09, Accepted 32023-07-31. https://doi.org/10.53234/scc202304/03

1. Introduction

The main goal of this paper is to challenge the IPCC's climate change science based on the AGW theory and to introduce the alternative climate change model NAGW, where naturally occurring changes have major roles.

The results of the IPCC are prevailing perceptions of global warming or more commonly climate change. According to AR6 (IPCC, 2021), the contribution of the anthropogenic climate drivers is 99.2 % of the global warming from 1750 to 2019. The model-calculated surface temperature Ts according to AR6 in 2019 was 1.27 °C and the estimate of the global observed temperature in 2019 was 1.29 °C (IPCC, 2021, Fig. 7-51). At first sight, it looks like there is a perfect match between the AGW and the observations. A prompt analysis reveals contradictions.

There is a significant improvement in the model calculated Ts values if compared to the same figures reported in AR5 (IPCC, 2013). The total Radiative Forcing (RF) was 2.34 Wm^{-2} in 2011. Using the Climate Sensitivity Parameter (λ) value of 0.5 K/(Wm^{-2}), the model calculated temperature Ts increase was 1.17 ºC. This figure is 37.6 % greater than the observed temperature of 0.85

ºC in 2011. The temperature value in 2019 was 1.29 °C. The reasons for this abrupt temperature increase should be identified since GH gases are not able to cause such a change in eight years only according to the IPCC.

The testimony of Christy (2017) in the U.S. House Committee on Science 2017 contains the description of the scientific test between the 102 CMIP5 climate model runs (CMIP5 means Coupled Model Intercomparison Project Phase 5 experiment design) and the tropical mid-tropospheric temperature from 1979 to 2016. The observed temperatures consist of satellites, balloons, and model-computed temperatures called reanalyze. The test applied the F-Test method of Vogelsang-Franses designed for determining whether the trends of the two time-series are equivalent or significantly different. The test values showed that all three observational temperature trends were highly significantly different (99 % confidence level) than the average of 102 CMIP5 models. The deviation between the average 102 CMIP5 models and the satellite temperature was about 0.55 ºC during the period from 2010 to 2015.

Together, 16 scientists have published an article (Santer et al., 2017) in which they realize that "*Over most of the early twenty-first century, however, model tropospheric warming is substantially larger than observed; warming rate differences are generally outside the range of trends arising from internal variability.*"

The first objective of this review study is to review the anthropogenic contributions to climate change in a way that an average reader can follow theories and conclusions. The most important issues are the RF magnitude of CO_2, the positive water feedback, transient climate response (TCR), and the relative strengths of greenhouse (GH) gases.

The second objective is to analyze the anthropogenic carbon quantity in the atmosphere and its residence time, which are the basis for the scenario calculations during this century.

The third objective is to analyze the GH effect specification of the IPCC, which is "IPCC-made" and conflicts with the IPCC policy that they apply only to reviewed research results. There are alternative specifications not considered by the IPCC. The GH effect specification of the IPCC does not affect global warming calculations, but it creates a strong GH gas image for CO_2.

The fourth objective is to introduce natural climate drivers, which are needed for explaining modern warming. The IPCC omits almost totally the long-term solar radiation changes, cosmic forces, and multidecadal, century- and millennial-scale oscillations as drivers of global warming.

The fifth objective is to summarize and analyze the differences between AGW and NAGW.

2. Materials and methods

The material and data applied to the IPCC reports and mainly the newest AR6 (IPCC, 2021) constitute the reference basis for analyses. The scientific papers, which may not have been referred to by the IPCC, constitute another source of results and data. The approach of this review study is to analyze critically the results of the IPCC and to compare them to the alternative research papers, which we could call research studies of contrarians. The RF value of CO_2 and the positive water feedback have decisive roles in the IPCC science and therefore these issues have been analyzed thoroughly.

3. Results

3.1 The strength of carbon dioxide (CO_2) as a GH gas

The RF value calculated at the tropopause was called instantaneous radiative forcing (IRF) in the AR5, and at the top of the atmosphere (TOA), the IPCC (2013) used the term Effective Radiative Forcing (ERF). The IPCC changed the terminology and the specifications of RF terms in the AR6

(IPCC, 2021). The Instantaneous Radiative Forcing (IRF) was defined now as the change in the net TOA (Top of the Atmosphere) radiative flux following a perturbation, excluding any adjustments. The Stratospheric Temperature-adjusted Radiative Forcing (SARF) was defined as the change in the net radiative flux at the TOA following a perturbation, including the response to stratospheric temperature adjustments.

The ERF is the final RF at the TOA for a particular forcing agent, and it is the sum of the IRF and the adjustments. The AR6 refers to four RF studies, which have practically the same ERF results but essential differences in calculation methods. The RF value caused by doubling the CO_2 concentration from 280 ppm to 560 ppm has been marked as $2xCO_2$ and it is needed in calculating climate sensitivity values as temperature changes. The $2xCO_2$ of Myhre et al. (1998) is 3.7 Wm^{-2} calculated by a logarithmic equation

$$RF = k \cdot \ln(C/560)\ [Wm^{-2}], \quad (1)$$

where k = 5.35, and C is the concentration of CO_2 (ppm). It should be noticed that RF is radiative forcing change due to the external climate driver changes, which may have happened since 1750. It is based on spectral calculations at the tropopause (3.55 Wm^{-2}) adding the stratospheric adjustments of 0.16 Wm^{-2}, which is 4.5 % of the ERF value. The ERF value of 3.7 Wm^{-2} has been used by the IPCC in three previous Assessment Reports, namely TAR (IPCC, 2001), AR4 (IPCC, 2007), and AR5 (IPCC, 2011). In 2010 Schmidt et al. (2010) called this value a canonical estimate as it seemed to be unchallenged.

In AR6 the IPCC writers introduced a higher $2xCO_2$ on questionable rationale. In the AR6 three other $2xCO_2$ values have been referred to, namely the 3.75 Wm^{-2} of Etminan et al. (2016) and the 3.75 Wm^{-2} of Meinshausen et al. (2020) are based on spectral calculations at the TOA by using the Oslo LBL code (Myhre et al., 2016). The $2xCO_2$ of Smith et al. (2018) the 3.70 Wm^{-2} and is based on the simulation of 11 GCMs applying the average IRF values at the TOA and the adjustments.

Finally, the IPCC (2021) formulated a new presentation not found in these referred scientific papers, since they replaced IRF with SARF. The IPCC formulated a new paradigm, and the ERF of 3.93 Wm^{-2} is 5.3 % greater than in the three referred studies above from 3.7 Wm^{-2} to 3.75 Wm^{-2}.

The analyses of the ERF values reveal that the ERF value of AR5 is a combination of the IFR value of 3.55 Wm^{-2} plus stratospheric cooling of 0.16 Wm^{-2} totaling 3.71 Wm^{-2}. The ERF of AR6 is a combination of an IRF value of 2.6 Wm^{-2} plus stratospheric cooling of 1.18 Wm^{-2} (Table 7.3). The IPCC does not pay any attention to these significant differences but reports that the ERF value is estimated to be at a “high confidence” level (AR6, p. 945).

There are different $2xCO_2$ values, which are not referred to in the AR6 (IPCC, 2021). Barrett et al. (2006) and Schildknecht (2020) have applied LBL (line-by-line) calculations and their values are 3.1 Wm^{-2} and 3.0 Wm^{-2}. Wijngaarden and Happer (2020) achieved a $2xCO_2$ value of 3.0 Wm^{-2} based on their LBL calculations using the HITRAN database (2021). Their RF value for $2xCO_2$ (from 400 ppm to 800 ppm) of 3.0 Wm^{-2} is at the altitude of 86 km, and the same value at 11 km is 5.5 Wm^{-2}, which has not been explained.

Harde (2013) also applied his own LBL calculations and his two-layer atmospheric model. His $2xCO_2$ value is 2.4 Wm^{-2}. Miskolczi and Mlynczak (2004) carried out extensive LBL calculations

with different atmospheric compositions, and their $2xCO_2$ value is 2.53 Wm^{-2}.

Ollila (2014) has reported a $2xCO_2$ of 2.16 Wm^{-2} utilizing LBL calculations with the Spectral Calculator tool (GATS, 2021) by using the HITRAN (2021) database and water-continuum model. Ollila's calculations are in line with Ohmura (2001) that 98 % of total LW absorption happens in the troposphere, and therefore the CO_2 absorption does not increase in the stratosphere, but it is saturated before the altitude of 1 km. The IRF value (the RF at the troposphere) of Smith et al. (2018) is 2.6 Wm^2.

3.2 Positive water feedback

Positive water feedback is a cornerstone in any GCM and the simple model of IPCC. IPCC (2007) writes in AR4 that *"The positive water feedback doubles the radiative forcing of any GH gas."* The AR5 (IPCC, 2013, p. 667) writes *"Therefore, although CO_2 is the main control knob on climate, water vapour is a strong and fast feedback that amplifies any initial forcing by a typical factor between two and three."*

The theoretical justification of positive water feedback is based on the equation of Clausius–Clapeyron. This equation represents the pressure-temperature relationship in a saturated water vapor atmosphere. The real atmosphere is not saturated by water vapor, and therefore the theoretical basis is weak. Because the atmosphere's saturation is around 70% on average, one could think that the positive water feedback relationship would follow the Clausius–Clapeyron equation anyway. The direct humidity and temperature measurements from 1980 onwards show no positive water feedback in the long run.

The temperature according to the UAH satellite data set of the lower troposphere (UAH, 2022) and absolute humidity as Total Precipitable Water (TPW) values from NOAA's NCEP/NCAR Reanalysis dataset (2022) is depicted in Fig. 1.

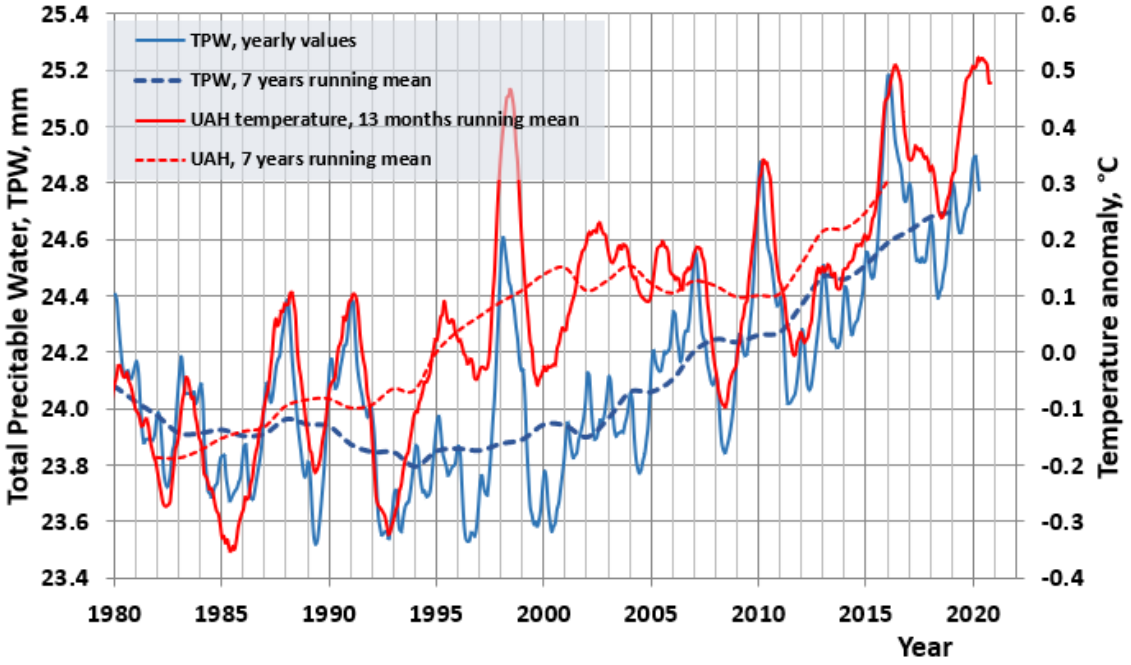

Figure 1: The temperature trend and TPW (Total Precipitable Water) trends from 1980 to 2020.

The short-term temperature changes are distinctly related to the El Niño and La Niña events, which are caused by the regional changes of the ocean currents and winds in the tropical central and eastern Pacific Ocean. They initiate the temperature change, and the strong change in absolute humidity amplifies the change by a factor of about 100 percent (Ollila, 2020a). It is practically the same as the positive feedback used by IPCC, but can it be found in the long-term trends?

There are essential features in the long-term trends of temperature and TPW, which are calculated and depicted as yearly and 11-year running mean values. The long-term value of temperature has increased by about 0.4 ºC from 1979 to 2000 but the TPW values show a negative trend. During the temperature pause from 2000 to 2015, the TPW values show a positive trend. This behavior of TPW conflicts with the positive water feedback theory.

The surface temperature values can be calculated using a simple equation, as defined by the IPCC (2013, p. 664):

$$dTs = \lambda \cdot RF \ [°C], \quad (2)$$

where dTs is the global mean surface temperature change, and λ is the "climate sensitivity parameter". The IPCC reported in TAR (2001) that "*λ is the nearly invariant parameter (typically about 0.5 K/(Wm^{-2}).*" This λ value was taken from the study of Ramanathan et al. (1985), based on eight research papers varying from 0.47 K/(Wm^{-2}) to 0.53 K/(Wm^{-2}).

When Syuruko Manabe was awarded the Nobel Prize for Physics in 2021, one of Manabe's main credits was that he was the first to introduce positive water feedback in 1967 (Manabe, 1967). He concluded that water feedback doubles the original RF of CO_2, and his λ value was 0.53 K/(Wm^{-2}). This feature became one of the essential features of GCMs as early as the 1980s but in his original paper, Manabe did not conclude if positive water feedback should be used or not in warming calculations.

In AR6 (IPCC, 2021) the IPCC changed its nomenclature and used the term "climate feedback parameter" α, which is the reciprocal of λ = 1/α. The feedback parameter α can be decomposed into different types of feedback, and the sum of feedback parameters is the direct relationship between the ERF and the global equilibrium surface temperature change.

Even though the IPCC did not report a λ value for ERF in AR6, it can be calculated from the data in Fig. 7.6 and Fig. 7.7 of AR6 (IPCC, 2021), which are based on the GCM calculations. The ERF value of 2.70 Wm^{-2} results in a warming of 1.27 °C, meaning the λ value of 1.27 °C / 2.70 Wm^{-2} = 0.47 °C/(Wm^{-2}), which is applicable in TCR calculations since the λ value of CO_2 is the same. This λ value means that water feedback has been applied in the GCMs used for calculating warming values in Fig. 7.7.

It is possible to calculate the value of λ using different methods. The simplest method is based on the total energy balance of the Earth by equalizing the absorbed and emitted radiation fluxes (Schlesinger, 1986; Ollila, 2014)

$$SC(1-\alpha) \cdot (\pi r^2) = sT^4 \cdot (4\pi r^2) \ [Wm^{-2}], \quad (3)$$

where SC is the solar constant (~1360 Wm^{-2}), α is the total albedo of the Earth, s is the Stefan-Boltzmann constant (5.6704*10^{-8}), and T is the temperature (K). The term SC(1-α)/4 is the same as the net radiative forcing (RF) and therefore Eq. (3) can be written in the form RF = sT^4. When

this equation is differentiated it will be $d(RF)/dT = 4sT^3 = 4(RF)/T$. The ratio d(RF)/dT can be inverted, transforming it into λ:

$$dT/(d(RF)) = \lambda = T/(4RF) = T/(SC(1-\alpha))\ [K/Wm^{-2}], \quad (4)$$

Using the average radiation CERES (2021) flux values for the period 2008–2014, λ = 255.3 K /(1360.04*(1-0.2916) Wm^{-2}) = 0.265 K/(Wm^{-2}). Temperature 255.3 corresponds to the Stefan-Boltzmann temperature for radiation 240 Wm^{-2}. Since λ gives the slope of a very nonlinear expression of temperature in the potency of four, there might be doubts if temperature change depends linearly closely enough on the RF. The maximum range of RF is +8.5 Wm^{-2} needed in the SSP5-8.5 Shared Socioeconomic Pathways (SSP) scenario calculations of the IPCC. In Fig. 2, the emission temperature is depicted as a function of the Stefan–Boltzmann law and according to Eq. (1), using the λ value of 0.265 Wm^{-2}. The deviation between these two curves is insignificant, and the numerical values show that in the RF range from 230 Wm^{-2} to 250 Wm^{-2}, the difference between these two equations is only 0.05 °C. This means that the linear Eq. (1) using a constant λ value is sound when calculating the dT values of different RF forcings.

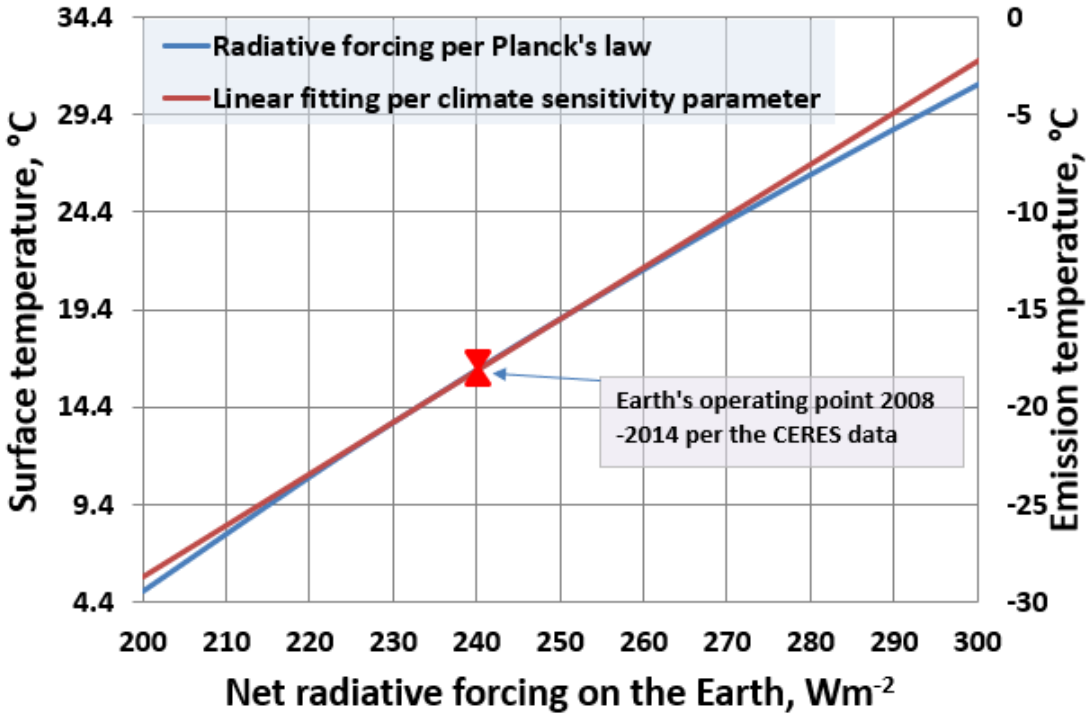

Figure 2: Emission temperature dependency according to Stefan-Boltzmann law and according to linear dependency per Eq. (4).

The difference between the λ values of 0.47 K/(Wm^{-2}) and 0.265 K/(Wm^{-2}) is due to the positive water feedback.

3.3 Climate sensitivity

Climate sensitivity (CS) is a useful measure, telling us how much the Earth's surface temperature Ts would increase if the CO_2 concentration would increase from 280 ppm to 560 ppm (=2xCO_2). There are two types of climate sensitivity, namely Transient Climate Response (TCR) which was called earlier Transient Climate Sensitivity (TCS), and Equilibrium Climate Sensitivity (ECS) (IPCC, 2013). According to AR6 (IPCC, 2021) the "*TCR is a surface temperature response for*

the hypothetical scenario in which atmospheric carbon dioxide (CO_2) increases at 1% yr^{-1} from pre-industrial to the time of a doubling of atmospheric CO_2 concentration (year 70)". The TAR of the IPCC (2001) defines TCR as a transition of the surface-troposphere system from one equilibrium state to another.

In the ECS calculations, the climate system must reach equilibrium, which takes a very long time, because the deep oceans are included and they need a long time to heat up, and not all feedbacks are developed into full effects, like albedo changes of the surface for example. IPCC (2013, p. 1112) also states that *"TCR is a more informative indicator of future climate than ECS"*. Therefore, the analyses of this study have been carried out only for TCR values.

Applying Eq. (2) gives the TCR value of 1.85 °C (= 0.47 °C/(Wm^{-2}) *3.93 Wm^{-2}), while the best estimate of AR6 (IPCC, 2021) is 1.8 °C. For example, the Ts for the worst-case scenario SSP5-8.5 determined according to Eq. (1) would be: dTs = 0.47 K/(Wm^{-2}) * 8.5 Wm^{-2} = 4.0 °C using the λ value of the AR6. Ts would be 4.5 °C using the λ value of 0.5 K/(Wm^{-2}), which is practically the same as the average value of 4.4 °C of the AR6 calculated by GCMs. These examples show that the average warming values calculated using Eq. (1) are the same as the results calculated by complicated GCMs applicable for the present-day warming, TRC calculations, and scenarios according to SSP calculations.

This fact is not easily accepted by those researchers who think that these calculations can be correctly carried out only by GCMs. What is the relationship between the λ and the TRC, and are the TRC values calculated using λ close enough to TRC values as defined by the IPCC?
It is a question about the dynamic delays in Ts calculations. The TCR specification (IPCC, 2021) defines that CO_2 increases at 1% yr^{-1}, from pre-industrial levels to double the atmospheric CO_2 concentration. Since the CO_2 growth rate has been smaller than 1 % yr^{-1}, the dT effects from 1750 to 2019 in Figure 7.7 of AR6 can be simply calculated according to the equation T = λ * RF. This means that the results are the same when using Eq. (1) compared to the average results of several GCM simulations. The same applies to TCR calculations, as shown above: 1.85 °C using λ versus 1.8 °C using GCMs. If there were time delays in response longer than one year, the equation dT = λ * RF would give different results.

One could expect, that the TRC values calculated by GCMs are more accurate than those calculated by using Eq. (1). In fact, there is quite a significant uncertainty range by using GCMs as can be found in the AR6 (IPCC, 2021): "*The best estimate of TCR is 1.8°C, the likely range is 1.4°C to 2.2°C"*. This uncertainty comes from the GCMs, which use different modeling methods and especially different quantities of various feedback. It means that GCMs do not improve the accuracy of TCR calculations but increase uncertainty for the reasons commented above.

Using Eq. (1) for calculating the warming values is justified since the dynamical time constant for the ocean is 2.74 months, and for land, 1.04 months (Stine et al., 2009). These values mean that for a stepwise RF change, Ts has reached its new equilibrium value in one year, since the settling time (also called relaxation or adjustment time, which means that 98.3 % of the final change achieved) is four times longer than the residence time (4 * 2.74 = 11 months) according to process dynamic system with one time constant. Sometimes a half lifetime has also been used, which means the time when 50 % of the change has happened and is mathematically in the first-order system = 0.693 * residence time.

The literature survey of non-IPCC TRC values can be divided into three major categories based on the research method, namely A) using the $2xCO_2$ values of the IPCC, B) using the $2xCO_2$ by applying researchers' own LBL analysis calculations, C) using observed Ts values and other climate data.

The TRC values of category A are very consistent being very close to each other: 1.15 °C from Bengtson and Schwartz (2012), 1.2 °C from Schlesinger (1986), and 1.33 °C from Lewis and Curry (2015). Even though these research studies apply 3.7 Wm^{-2} as the RF value, they have not found positive water feedback in the climate explaining the deviations from the IPCC's value of 1.8 °C. These results are fully in line with the IPCC (2007), which writes in section 8.6.2.3 of AR4 that *"with no feedback operating, the global warming from GCMs would be around 1.2 °C."* Ollila (2020b) has carried out warming calculations by applying only feedback from the atmosphere, which is called Planck's response. Using an RF value of 3.7 Wm^{-2} gives the warming value of 1.12 °C, which is also very close to the values above.

The results of category B vary considerably little: 0.6 °C by Barrett et al. (2006), 0.48 °C by Miskolczi and Mlynczak (2004), 0.51 °C by Ollila (2012), 0.6 °C by Ollila (2014), 0.5 – 0.7 °C by Kissin (2015), 0.4 °C by Smirnov (2017), 0.7 °C by Harde (2017), and 0.5 °C by Schildknecht (2020). The only explanation is that these researchers have found a smaller $2xCO_2$ value than 3.7 Wm^{-2} and they have not found positive water feedback. The differences cannot be explained by the identified flaws in calculation methods.

The survey of research studies of category C reveals that the TRC values vary from 0.0 °C of Fleming (2018) to 1.2 °C of Otto et al. (2013). The results of this category are not reliable enough since they are too heavily dependent on other climate drivers like solar irradiation variations, volcanic impacts, surface albedo changes, etc. Kissin (2015). Usually, the elimination of these effects has not been considered at all.

It should be noticed that the survey of this study does not cover all research studies showing lower CS values than IPCC. Gervais (2021) has listed 109 studies that conclude that CS is from 0.0 to 1°C. The most common result of these studies is that the TRC/ECS value is negligible or close to zero, and they are usually based on the analysis of empirical climate data. The studies of Miskolczi (2014) and Drotos et al. (2020) have proposed a feedback mechanism in the climate that will drive the long-term temperature effect of $2xCO_2$ to zero, which means that the GH effect would be constant and not depend on the CO_2 concentration.

3.4 Relative strengths of major GH gases

The global warming potential (GWP) definition means how much 1 kg GHG can absorb infrared energy if it has been released into the atmosphere over a specified period (normally 100 years) when compared to the same quantity of CO_2 gas (IPCC, 2007). The 100-year GWP value of methane is 27.9 and the same value of nitrogen oxide is 273 (IPCC, 2021). The GPW value definition is highly theoretical, and it is not applicable in warming calculations, because only the actual GH gas concentration has a warming impact and not the future concentrations.

A more realistic analysis can be carried out to identify the relative strengths in the climate of this century by increasing the GH gas concentration in question by 10 % from its concentration in the present atmospheric conditions and calculating the absorption for the altitude of 120 km (Ollila, 2017a). When CO_2 acts as a reference having a strength of 1, the relative strengths of other GH gases are water vapor 11.8, ozone 0.78, nitrogen oxide 0.14, and methane 0.11,

The simplest method for comparing the relative strengths of GH gases is to compare their RF

values from 1750 to 2019 as shown in Table 1.

Table 1. Relative strengths of carbon dioxide, methane, and nitrogen oxide according to AR6 (IPCC, 2021, Fig. 7.6) based on the concentration changes from 1750 to 2019.

GH gas	*RF in 2019* Wm^{-2}	*Concentration change* %	*RF per 1 % change*	*Relative strength*
CO_2	2.16	40.36	5.35	1
CH_4	0.54	159.17	0.34	0.11
N_2O	0.21	20.00	1.05	0.25

These two calculation methods show that the GWP values give wrong impressions of GHG strengths, and they do not represent the warming impacts of GHGs in a certain year during this century. The warming impact of water vapor is almost linearly dependent on the water vapor content in the atmosphere, and it explains why water is such a strong GH gas.

The physical explanations for these relative strengths can be noticed in Fig. 3, where the absorption peaks of major GH gases have been depicted applying line-by-line (LBL) calculations (Gats, 2014), and HITRAN (2021) data base.

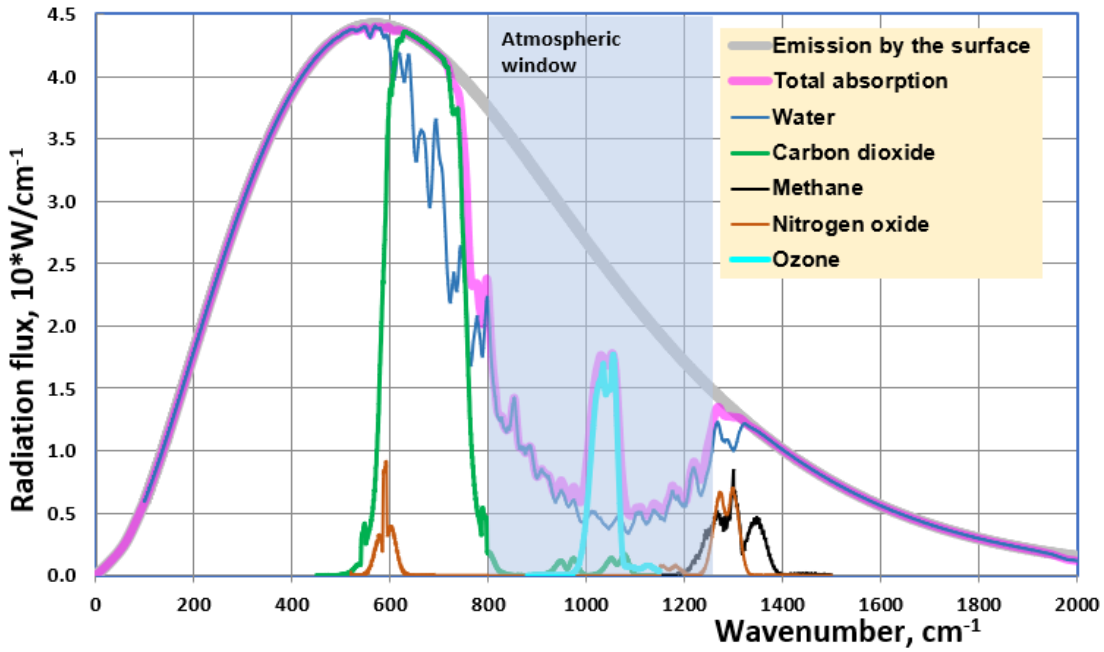

Figure 3: The absorption areas of GH gases in clear sky conditions.

The absorption peaks of methane and nitrogen oxide are badly overlapping with the absorption effects of water and carbon dioxide explaining their weak RF impacts. On the other hand, the absorption peak of ozone is relatively strong since in its absorption wavenumber zone from 1000 to 1100, water has the minimum absorption effect.

3.5 Carbon dioxide circulation and time delays in the atmosphere

In calculating the future warming impacts of CO_2, it is important to know in which way fossil fuel-based missions would change the atmospheric CO_2 concentration. The only way to identify his

behavior is to build a model simulating the carbon cycle between the atmosphere, the ocean, and the land. About 25 % of the atmospheric CO_2 changes every year, because the oceans absolve and dissolve CO_2, and in the same way land plants (later land) photosynthesize and respire CO_2. The present-day anthropogenic emission of about 10 GtC per year (gigatons of carbon) is only 4.5 % of the annual CO_2 flux of about 220 GtC circulating through the atmosphere, Figure 4.

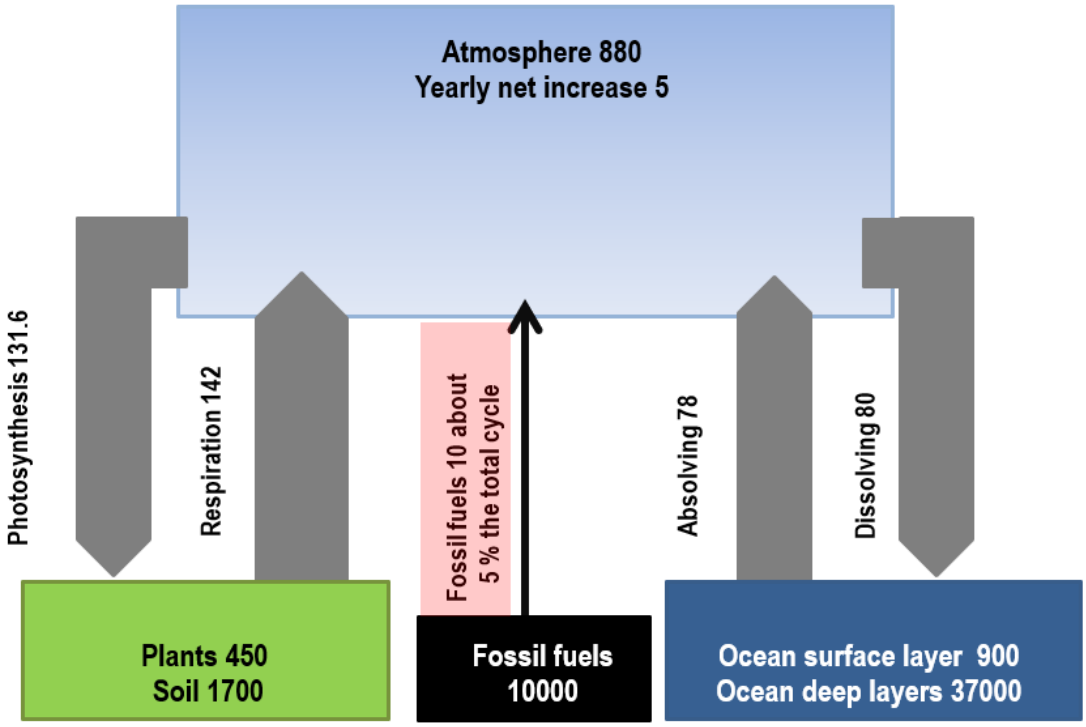

Figure 4: The carbon cycle presentation shows the recycling flux values of the IPCC (2021, Figure 5.12). The numerical values are reservoir amounts in gigatons of carbon (GtC); the flux values are in GtC yr^{-1}.

Since 1960, CO_2 circulation has behaved practically the same way. The fossil fuel emissions have been about 10 GtC and the atmospheric CO_2 increase has been 5.5 GtC. Even though it looks like 55 % of the annual fossil fuel emissions stay in the atmosphere, it does not mean that this increase is totally anthropogenic as the IPCC assumes. Yearly fossil emissions mix with the existing atmospheric CO_2. From this almost evenly mixed CO_2, the ocean, and the land uptake CO_2 according to their atmospheric composition, and simultaneously CO_2 flows into the atmosphere from the ocean and the land having different compositions.

A comprehensive isotope measurement study of the dissolved CO_2 in the ocean (Sabine et al., 2004) shows that the ocean is a sink for the anthropogenic CO_2, but the sink of the total CO_2 (total CO_2 is the mixture of anthropogenic and natural CO_2) between the ocean and the land is not clear. The ocean is the main sink also for the total CO_2 (IPCC, 2013; Ollila, 2020c). This means that if the recycling system of CO_2 works in the same way also during this century as well, the atmospheric CO_2 concentration increases steadily.

Two permanent isotopes of carbon molecules exist. The most common is ^{12}C, having 6 positrons and 6 neutrons; however, ^{13}C has one extra neutron. Isotope ^{12}C is the most common, being 98.9 % of all carbon; the rest is ^{13}C. An exceedingly small concentration of unstable isotope ^{14}C, which is radioactive, also exists.

The measurement unit of ^{13}C (marked as $\delta^{13}C$) is a fraction of carbon isotope ^{13}C expressed as ‰, and it has been called permille. This unit is linearly dependent (Srivastava et al., 2018) on the relationship $^{13}C/^{12}C$:

$$\delta^{13}C = (S/N-1) \cdot 1000\ [‰], \quad (5)$$

where $S = {}^{13}C/^{12}C$ being a sample and $N = (^{13}C/^{12}C)_{standard} = 0{,}0112372$. Many climate researchers have never heard about this measurement unit. It looks like the IPCC does not want to report on permille values since in the AR6 (IPCC, 2021) there is only one figure namely Fig. 5-6 and its panel c, where there is a short permille trend of the atmospheric CO_2. The same applies to the main referred research study (Friedlingstein et al., 2020), which is the basis of the carbon cycle description in the AR6: no reference to the permille values.

Anthropogenic CO_2 means CO_2 originating from fossil fuels and land use (NOAA, 2018). Fossil fuels have the same permille value as plants from the Carboniferous era (359 – 299 million years ago); this value is -28 ‰. The typical $\delta^{13}C$ values in the present day are the atmosphere about -8.6 ‰, the ocean surface from -8.0 ‰ to -10 ‰, the land -26 ‰, and the fossil fuels -28 ‰ (Quay et al., 2003; NOAA, 2018).

The term "total CO_2" has been used for the mixture of natural and anthropogenic CO_2 flux or quantity. The Suess Effect shifts continuously the isotopic ratio of both ^{13}C and ^{14}C in the atmosphere and the ocean because of anthropogenic CO_2 emissions.

Carbon cycle models referred to by the IPCC are all-encompassing and they apply several submodels designed for special tasks like CO_2 exchange with plants. In this section, the approach is to analyze critically the IPCC's carbon cycle model, which refers to the yearly published article "Global Carbon Budget" by Friedlingstein et al (2020), and to compare its key figures to the results of the 1DAOBM-3 model of Ollila (2020c), and Berry (2021).

In AR5, the IPCC (2013a, p. 467–469) writes: "*About half of the emissions remained in the atmosphere 240 PgC±10 PgC since 1750.*" In the same way in AR6 (2021), the increased mass of the atmosphere originates from the emissions. The total CO_2 mass in 2019 is 876 GtC; in 1750, the same was 591 GtC (IPCC, 2021). Three simple tests can be carried out to check the numbers of the AR6. If the total CO_2 increase were anthropogenic CO_2 as IPCC reports (2021), its quantity would be 285 GtC in 2019, meaning a fraction of 32.5 %. The rest (67.5 %) would be assumed to be natural CO_2 having a $\delta^{13}C$ value of -6.35‰, which is the permille value of the atmospheric CO_2 in 1750. The $\delta^{13}C$ of this atmospheric CO_2 mixture would be

$$\delta^{13}C = 0.324 \cdot (-28) + 0.676 \cdot (-6.35) = -13.4\ [‰] \quad (6)$$

If eq. (6) would give the permille value of -8.6 ‰, the permille value of the natural CO_2 in the atmosphere should be about +1.0 ‰. Since the plants have not acted as a sink according to AR6 (IPCC, 2021, p. 5-22), the land has not changed the atmospheric permille value. The ocean has been the major sink but the fractionation from air to sea and from sea to air are so close to each other that the recycling fluxes have not been able to change the natural CO_2 value significantly. This analysis shows that the increased atmospheric mass from 1750 cannot be totally anthropogenic since the currently observed $\delta^{13}C$ is about -8.6‰.

Another test can be carried out to test the correctness of the carbon cycle figures of the IPCC (2021). There is a fractionation phenomenon from air to sea, from sea to air, and vegetation CO_2 exchange. However, about 99 % of anthropogenic CO_2 is a carbon isotope of ^{12}C; therefore,

its recycling happens similarly to natural CO_2. Although the ^{13}C fraction would differ in recycling anthropogenic carbon fluxes, over 99 % is the same substance, which must still be labeled anthropogenic if it originates from human actions. Table 2 has enlisted the carbon cycle fluxes (CCFs) of the IPCC (2021) from Fig. 5.12 since it is the only presentation of this kind in the AR6.

Table 2. The average CCFs (GtC yr^{-1}) from 2010 to 2017, according to IPPC (2021, Fig. 5.12), and the percentage fraction of the anthropogenic CO_2 from the total oceanic or terrestrial CCF.

CO_2 quantity/flux	Total CO_2	Anthropogenic CO_2	
	GtC / GtC yr^{-1}	*GtC*	*%*
In the atmosphere	870	279	32.1
From the atmosphere to the ocean	79.5	25.5	32.0
From the atmosphere to the land	142.0	29.0	20.4

The key figures in Table 2 mean that the ocean-atmosphere flux would not discriminate the atmosphere's anthropogenic fraction since this flux contains the same 32.0 % of anthropogenic CO_2 because in the atmosphere this fraction-% is almost the same as 32.1. Surprisingly enough, the gross photosynthesis flux has only 20.4 % of anthropogenic CO_2. Does a physical explanation for this land discrimination exist? No. Instead, the plants prefer anthropogenic CO_2 for its higher ^{12}C isotope concentration. The ocean's euphotic layer (max. depth of about 200 m) also favors anthropogenic CO_2 since phytoplankton and plants prefer the ^{12}C.

The fractionation phenomenon between the reservoirs changes the relative quantities of ^{13}C molecules (quantity only about 1.1 % of the total CO_2 mass) and it affects the permille number of the CO_2 quantity sequestrated by a reservoir. But fractionation does not control the sequestration process since it is only a consequence.

The AR6 (IPCC, 2021) does not report, in which way the anthropogenic CO_2 is divided between the ocean mixing layer and the intermediate & deep ocean. Gruber et al. (2019) reported that 50 % of the anthropogenic CO_2 is in the layer above 400 meters depth. The total anthropogenic CO_2 in the ocean was 160 GtC in 2019 (IPCC, 2021). Since the surface mixed layer depth is 75-100 meters, the anthropogenic CO_2 in this layer can be estimated to be about 0.3*0.5*160 = 25 GtC. According to IPCC (2021), the annual average recycle 2008-2017 flux of anthropogenic CO_2 was 25.5 GtC. These figures would mean that the ocean recycle flux would return yearly into the atmosphere practically all the anthropogenic CO_2, which was absorbed by the surface mixed layer. This would mean zero sequestration rate by the ocean. This is the third example of the physical contradictions of the IPCC model.

The main differences in carbon cycle representations between the AR6 of the IPCC (2021), which is based on the research report of Friedlingstein et al. (2020), Ollila (2020c), and Berry (2021) have been tabulated in Table 3.

Table 3. The key figures of anthropogenic CO_2 in the atmosphere according to Friedlingstein et al. (2020) from 2010 to 2019, Ollila (2020c) for the year 2019, and the same of Berry for the year 2020.

Quantity/flux	Cumulative 1750-2019 *GtC*			Yearly net fluxes *GtC yr^{-1}*	
	IPCC	Ollila	Berry	IPCC	Ollila
Anthropogenic CO_2 in/to the atmosphere	285	70	71	5.1	0.3
Anthropogenic CO_2 in/to the ocean	170	250	206	2.5	5.8
Anthropogenic CO_2 in/to land plants	230	166	71	3.4	3.2
Total anthropogenic quantity	685	496	452		

The total quantity of anthropogenic CO_2 of Ollila includes 32 GtC of land-use CO_2 emissions, and the same of the IPCC is 240 GtC (imbalance in terrestrial sink 10 GtC). The anthropogenic CO_2 quantities of Berry and Ollila are very close to each other, and the main difference is due to the land-use emissions applied by Ollila. This result is very interesting since the calculation basis of Ollila is a complicated physical model of CO_2 recycling between different reservoirs considering the fractionation between reservoirs and Berry's approach is simpler.

In tracer testing, which is commonly used in scientific studies, a very small quantity of a chemical or a radioactive compound is used to detect flows, delays, and other dynamic properties of a fluid system under scrutiny. For estimating the residence time of the anthropogenic CO_2 in the atmosphere, the results of the only full-scale test carried out by humanity with the climate are now available. The nuclear bomb tests in the atmosphere from 1945 to 1964 accidentally created this kind of tracer test situation.

The decay curve of the ^{14}C can be combined with some of the worldwide measurements (Levin et al., 2010; Utrecht, 2016; LLNL, 2016) carried out since the 1950s and this is illustrated in Fig. 5. The simulated decay rate of the first order dynamic system with a residence time of 16 years gives an excellent fit.

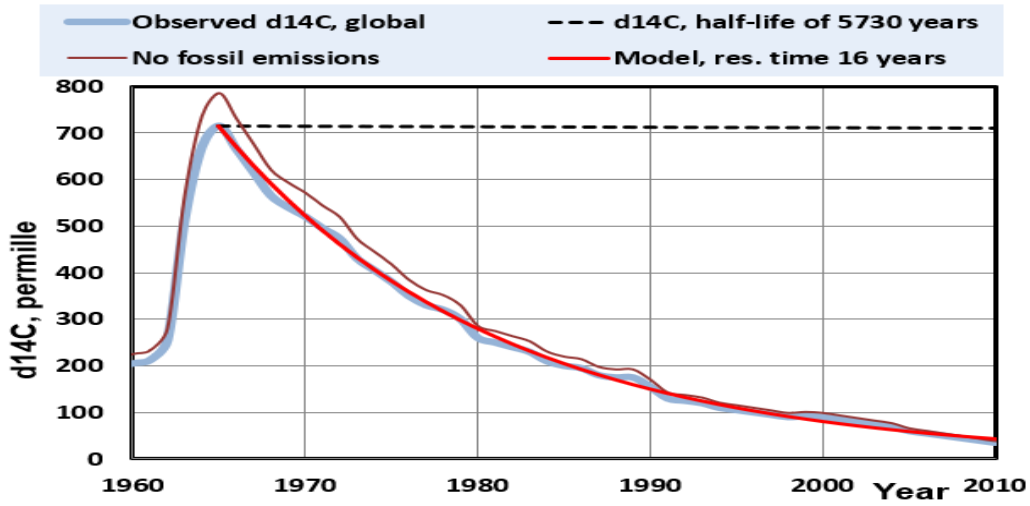

Figure 5: The observed global decaying rate of ^{14}C (blue curve), the simulation result by 1DAOBM-3 (red curve), the theoretical decaying rate of ^{14}C without recycling fluxes in the carbon circulation system (black dashed curve), and the estimated decaying rate in the climate system without fossil fuel emissions (brown

curve).

This tracer test by the ^{14}C corresponds perfectly to the behavior of anthropogenic CO_2. In both cases, the concentration change of a new CO_2 flux into the atmosphere starts from zero. The nuclear bomb test can be used to validate any CO_2 circulation model.

If a model gives a shorter residence time of 16 years for anthropogenic CO_2 in the atmosphere, it is probably wrongly composed. This is true for early research studies showing residence times from 2 to 15 years, which gives an average residence time is 7.6 years, which was identified by Segalstad (1998) when he surveyed 34 residence time studies from 1957 to 1990. A common feature of these studies is that they have used a model, where is one mixing tank (the atmosphere) and the total CCF flows through this tank. This process model is flawed since in reality, the carbon cycle encompasses three reservoirs with recycling fluxes.

Revelle and Suess (1956) estimated that "the exchange time" for an atmospheric CO_2 molecule to be absorbed by the sea is "the order of magnitude of 10 years". In this case "the exchange time" T_e was defined to be the half-life time since T_e was marked to be 1/k, where k is the time constant of the first-order dynamic system. A half-time means the time when 50 % of the change has happened. For the first order system a half time = ln2/k = 0.693/k. Residence time T is 1/k. Therefore, in the first order system $T_e = 0.693 * T$.

The value of 10 years of T_e by Suess and Revelle corresponds to 14.4 years of residence time. This value calculated from cosmogenic ^{14}C data is surprisingly close to 16 years of T confirmed by the empirical nuclear bomb tracer test years later.

Another useful timescale is relaxation time or adjustment time (marked with T_{adj}), which means the time needed for a perturbed system to return to equilibrium or a steady state. Because theoretically, T_{adj} would be infinitely long, in practice T_{adj} is approximated by multiplying the residence time by four: $T_{adj} = 4$ T. At this time moment, a step change has reached the level of 98.3 % from the final equilibrium value. The IPCC uses T_{adj} values in reporting how long it takes the anthropogenic CO_2 to leave the atmosphere if anthropogenic emissions would stop.

In AR5 the IPCC (2013, p.469) writes: "*The removal of human-emitted CO_2 from the atmosphere by natural processes will take a few hundred thousand years (high confidence). Depending on the RCP scenario considered, about 15 to 40% of emitted CO_2 will remain in the atmosphere longer than 1,000 years."* The conclusion about IPCC's adjustment time for anthropogenic CO_2 is that it is in direct conflict with the tracer test results with radiocarbon. The relaxation time of 1DAOBM-3 is 64 years is the same as the radiocarbon relaxation time.

The simulation results applying 1DAOBM-3 (Ollila, 2020c) and Berry (2021) show that the quantity of the anthropogenic CO_2 in the atmosphere in 2019 is only 70 GtC, corresponding to the portion of 8 % because natural CO_2 flows into the atmosphere from the ocean and the vegetation. According to Ollila (2020c), this quantity is concordant with the $\delta^{13}C$ measurement in 2017 (Locean, 2016) being -8.6 ‰. Any permille value observation or presentation and how it should be calculated cannot be found in the AR6 (IPCC, 2021) or Friedlingstein et al. (2020). The conclusion could be that the division between natural and anthropogenic atmospheric CO_2 quantity does not support the observed $\delta^{13}C$ value.

Harde and Salby (2021) have concluded that the residence times of atmospheric natural and anthropogenic CO_2 are the same since the CO_2 molecules are similar. They use the term "absorption time", which seems to be according to graphical presentations the same as the residence time of 16 years of bomb carbon.

A simple test can be carried out if the adjustment time of 64 years could be possible for the total CO_2 increase of 285 GtC to leave the atmosphere. How long it would take that the extra 285 GtC in the atmosphere would decrease to zero if the anthropogenic emissions (about 10 GtC yr^{-1}) would be stopped totally? If the yearly decrease would be the same as the present-day sequestration rate of about 4.5 GtC each year, it would take 63 years. But as the decay curve of ^{14}C shows in Fig. 5, the decay rate will decrease continuously according to the first-order dynamic model, which time constant is 16 years. The atmospheric anthropogenic quantity of 70 GtC can decrease to almost zero in 64 years as has happened but it is impossible to the total CO_2 stock of 285 GtC due to the restricted sequestration capacity of the ocean and the land plants.

The only way to find an answer is a model simulating carbon recycling between the three reservoirs. Ollila has simulated the decrease rate of the total atmospheric CO_2 when anthropogenic emissions stop by applying his model 1DAOBM-3 and the simplified dynamic models of Bern2.5CC (Joos et al., 2001) and Joos2013 by Joos et al. (2013). Bern2.5CC has been also the selection of the IPCC. The results have been depicted in Fig. 6.

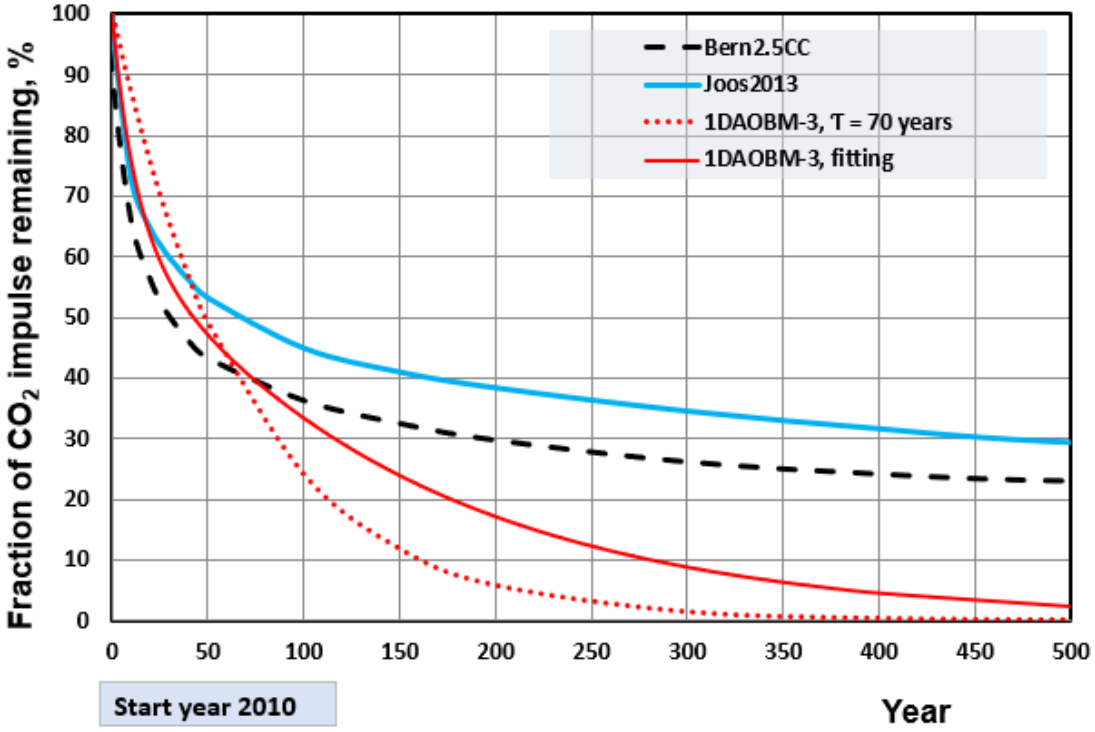

Figure 6: Decay rates of total atmospheric CO_2 concentration using different carbon cycle models.

The dynamic models of Bern2.5CC and Joos2013 are combinations of four first-order dynamic models with different residence times from 1.189 years to 393.4 years and a constant, which means that CO_2 would never decrease to zero level but stay at the level of about 20 % from the original starting level. There is no physical reason for this assumption.

The fitting of the 1DAOBM-3 simulation shows that a residence time of about 70 years is a reasonable compromise. It is not very good fitting since recycling fluxes, especially from the land, increases on a yearly basis with more and more CO_2 coming into the atmosphere. It means that the adjustment time would be 4*70 = 280 years before the atmospheric CO_2 level would have returned to about the same level as 1750. It is rather a coincidence that the present CO_2 concentration

increase has happened during the last 270 years. The surface temperature after 2010 in this simulation has been constant.

A common feature among the IPCC contrarians is that the increase in atmospheric CO_2 cannot be totally anthropogenic since they find several flaws and violations of physical laws in the IPCC's carbon cycle modeling. There are still different results among the research studies of the IPCC science opponents but they are coming closer to each other.

3.6 The decadal climate oscillations

The first observational evidence for about 60- to 80-year temperature oscillations in the North Atlantic basin was identified during the 1980s (Folland et al., 1984; Folland et al., 1986), and they were followed by Schlesinger and Ramankutty (1994), and Klyashtorin et al. (2009). This phenomenon was termed the Atlantic Multidecadal Oscillation (AMO) by Kerr (2000). Chen et al. (2018) identified the same kind of oscillation in the northern part of the Pacific, and it has been termed the Pacific Multidecadal Oscillation (PMO).

Researchers of astrophysics have studied the cyclic behavior of solar magnetic activity since 1843 when it was discovered by Schwabe (1843) to have about an 11-year duration. Hale (1908) discovered the magnetic nature of sunspots and that the complete magnetic cycle spans two solar cycles (22 years). Gleissberg found in 1958 that the solar cycles weaken and strengthen in the period of about 80 years by applying a lowpass filter to the sunspot number records. The periodicity of the 88-year Gleissberg cycle like the 220-year Suess (1980) cycle is related to the Schwabe cycle.

The same periodicities of about 60- to 90-year have been found in regional and global measurements and proxies during the thousands of years like the global temperature (HadCRUT5, 2021), Indian monsoons (Agnihotri et al., 2002), NE Pacific coast sediments (Patterson et al., 2004), cosmogenic isotope concentrations of ^{14}C and ^{10}Be (Attolini et al., 1987; Cini Castagnoli et al., 1992), auroral records (Feynman and Fougere, 1984), and tree-ring analyses (Lin et al., 1975; Peristykh and Damon, 2003; Ollila and Timonen, 2022). Scafetta (2010) and Ollila (2017b) have introduced and analyzed the planetary oscillation called Astronomic Harmonic Resonances (AHR), which creates a 60-year oscillation pattern. These different 60-oscillations have been depicted in Fig. 7.

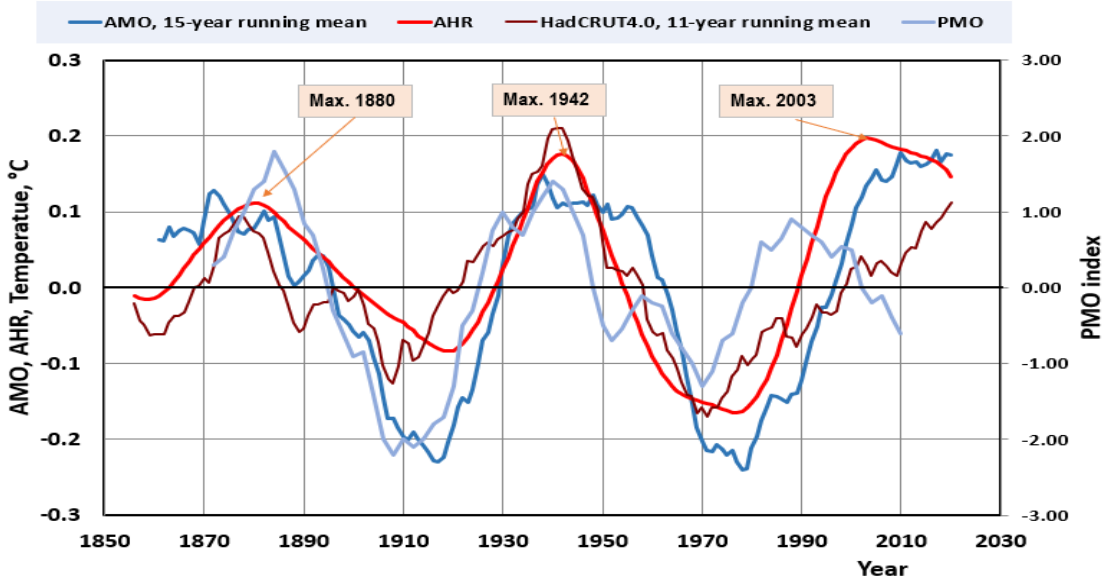

Figure 7: The 60-year fluctuations of AMO (NOAA, 2022), PMO, AHR, and temperature trends. The AHR trend is from the study of Ollila (2017b), and the PMO has been digitized from Fig. 5 of Chen et al. (2016) with 2-year steps.

As Fig. 7 indicates, the AMO and PMO are probably connected to global-scale multidecadal oscillation (GSMO), also called Global-Scale Multidecadal Variability of about 50 to 70 years as observed in the temperature behavior. The trends also illustrate the fact that the NH oscillations are stronger than global oscillation amplitudes.

Internal and external forces have been proposed to cause oscillations. The special group of explanations has found a connection to cosmic forces, like Ermakov et al., (2009). Scafetta (2010) and Ollila (2017b) have found that the orbital periods of Jupiter and Saturn can create temperature variations of 60 years by moving the solar system barycenter, which causes variations in the cosmic dust quantity entering the atmosphere. The temperature effect happens through cloudiness variations.

Ollila and Timonen (2022) analyzed the year-accurate tree-ring data series called the Finnish Timberline Pine Chronology (FTPC) from the year 1000 onward. They found that the tree-ring variations can be explained with two oscillation periods of 60- and 88-years. The 60-year period matches the AHR phenomenon, and the longer oscillation is a well-known 88-year Gliessberg oscillation. In Fig. 8 the 60- and 88-year cycles have been combined and the periodicity of the combined signal correlates very well with the FTPC tree-ring signal, Fig. 8.

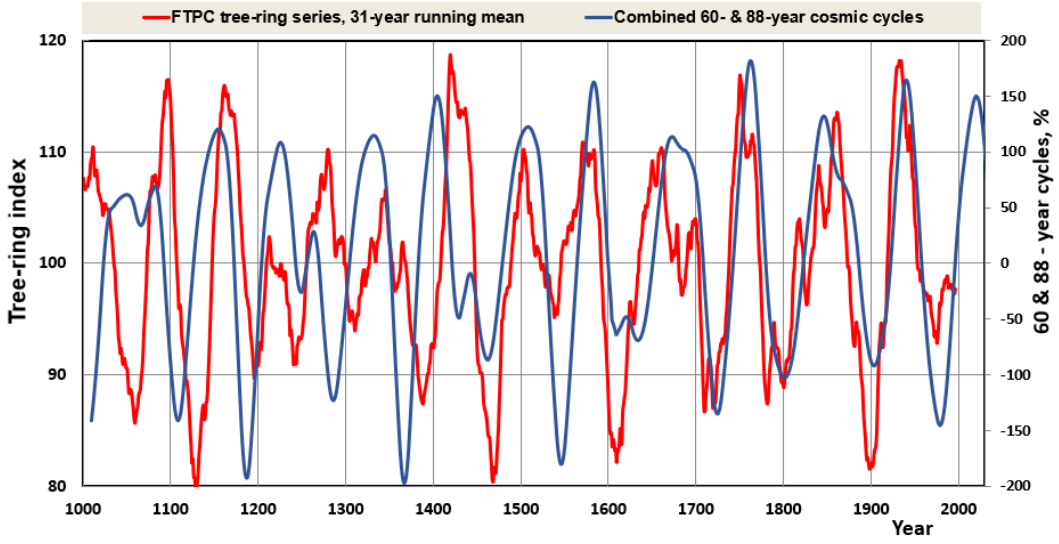

Figure 8: FTPC 31-year running mean signal and combined AHR & Gleissberg signal.

The temperature effect of the 60- & 88-year signal on the temperature change from 1750 to 2019 is minimal since there are grand maximums (simultaneous maximums) during these years. On the other hand, this oscillation can explain the cyclic behavior of the global temperature from 1750 to 2020.

The 60- to 88-year oscillations had their simultaneous maximums in 1940. When the oscillation phases changed to negative phases, the cooling effect of the 60- & 88- year oscillations became dominant over the greenhouse gas effects and caused global temperature to decrease, which happened from 1940 to 1975. Similarly, when the 60- & 88 oscillations turned from a negative to a positive phase, global warming accelerated, as it did after 1975, and finally increased the global temperature by about 0.25 °C (Fig. 6) till 2000. The IPCC has not recognized this temperature behavior in its temperature reconstruction during the 1900s.

3.7 Century- and millennial-scale climate oscillations

Century- and millennial-oscillations have a major role in explaining long-term variations thinking the anthropogenic period from 1750 to the present. If there are longer periodicities than about 250 years, they are possible explanations for the present-time warming, at least partially. The first step is to find out research studies analyzing these periods and the second step is to analyze the proposed mechanisms.

Century- and near-millennium scale research studies have typically used ice-core drilling samples of Antarctica and Greenland, and the other group of studies has used cosmogenic analyses of ^{14}C and ^{10}Be samples from other sources like marine and lake sediment records, and $\delta^{18}O$ records of speleothems (geological formations of mineral deposits in natural caves).

The analyses (Davis et al., 2017; Davis et al., 2018; Davis et al., 2019) of Antarctica drill hole samples have revealed a dominating periodicity of about 143-146 years during the last 446 millennium years, which has been coined to Antarctic Centennial Oscillation (ACO) and Antarctic Oscillation (AAO). The analyses show also millennial-scale oscillations from 800 to 1500 years.

The temperature and CO_2 variations are smaller in Antarctica than in Greenland, and therefore

the same oscillations should be easily found also on the Northern Hemisphere. Dansgaard et al. (1984) and Dansgaard et al., (1993) concluded from the ice-core records of Greenland for the period of 250 000 years that climate has been unstable during glaciation periods, and these climate periods were named Dansgaard – Oeschger (D-O) oscillations. The periodicities of Greenland's ice-core records according to Vinther et al. (2010) have been 1270, 1470, and 2550 years. In the later article of Vinther (2011), a dominant period is about 1000 years peaking at 1000 and 2000 years. Bond (1997) has found the same 1470±500 years periodicity in the North Atlantic Sea sediments during the Holocene.

Davis et al. (2019) have named external forces of the Earth like periodic variations in solar insolation and natural perturbations of Earth's orbital cycles to be probable reasons for variations. Also, Bond (1997) thinks that oscillations found in the North Atlantic area are caused by solar insolation changes.

3.8 The Sun's activity changes

The Earth receives about 99.97 % of its energy from the Sun. The Sun's radiated energy measure is Total Solar Irradiance (TSI), which has both long-term variations in the millennium scale and short-term variations like Schwabe's 11-year cycle and Gleissberg's 88-year cycle. Solar magnetic field variations are responsible for solar irradiation changes. There are two main categories of methods in evaluating historical TSI values, which are sunspot records starting from 1610 and cosmogenic isotopes of ^{10}Be and ^{14}C applicable for millennial periods.

Hoyt and Schatten (1993) have used the indices of the equatorial solar rotation rate, sunspot structure, decay rates of sunspots, the number of sunspots without umbrae, and the decay rate of sunspots and sunspot cycle, and developing a model for TSI calculation. Lean (1995, 2004, 2010) has reconstructed the TSI trend from 1610 onward by using revised sunspot activity records and the correlation between sunspot darkening and faculae brightening (bright areas between sunspots data). Bard et al. (2000) have used the cosmogenic isotope measurements of ice cores samples of the South Pole. These TSI constructions have been depicted in Fig. 9.

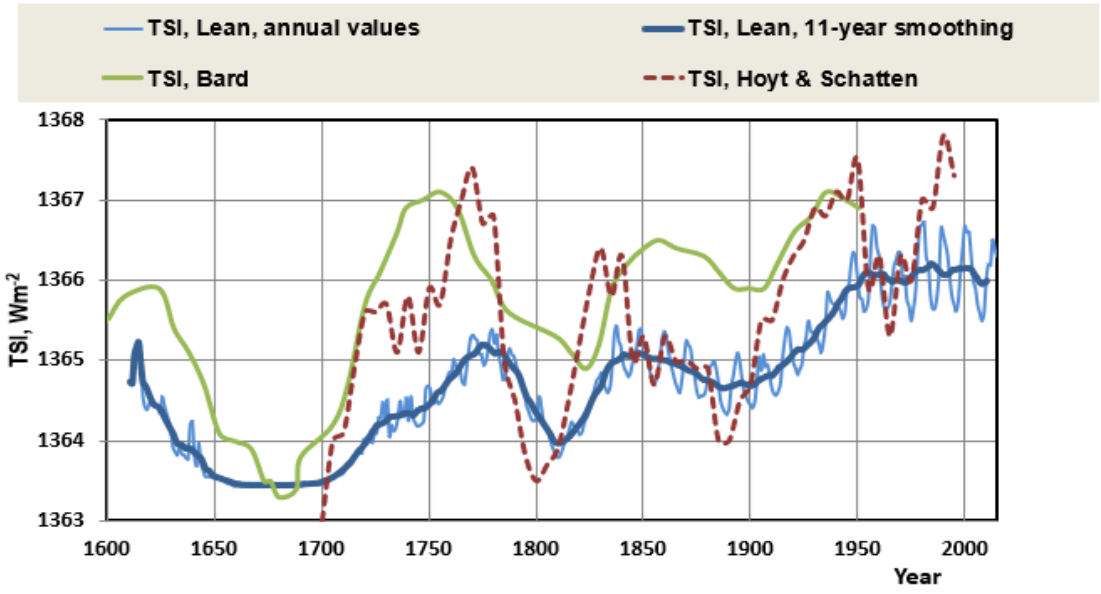

Figure 9: TSI reconstructions of Lean (2004), Hoyt and Schatten (1993), and Bard et al. (1997).

According to the data of Lean (2004), the estimated TSI change from 1750 to 2000 has been about 1.1 Wm^{-2}. Based on the latest TSI observations, Lean (2010) has modified her original TSI estimate of 1366 Wm^{-2} for the 2000s to the modern TSI level of 1361 Wm^{-2} but her estimate for the TSI change is the same 1.1 Wm^{-2}. This TSI change means an RF value of 1.1/4 = 0.275 Wm^{-2}. Connolly et al. (2021) have carried out a comprehensive review study about Sun effects on the Northern Hemisphere temperature trends. Its results show a common feature in all TSI reconstruction studies that around 1900 the TSI value was about -2 Wm^{-2} lower, in the 1930's about +1 Wm^{-2} higher, and from 1990 onward about 1.5 Wm^{-2} higher than the reference level. The TSI reconstruction of Velasco Herrera et al. (2015) shows the same general TSI trends as above and they also predict that the TSI trend has a minimum of around the 2050s.

A general conclusion can be drawn that the TSI has varied from 1600 onward including low TSI values during the Little Ice Age (LIA, Maunder minimum 1645 - 1715) and Dalton minimum (1790 – 1830). The Sun's activity seems to be now at the maximum level starting from 1990 and the TSI value has varied thereafter relatively little according to the Sun's cycle phase of about 11 years (Schwabe cycle).

Kauppinen et al. (2010) and Ollila (2013) have found from satellite cloudiness observations that a 1 % cloudiness change causes a 0.1 °C temperature change. Ollila (2017b) has introduced that the TSI impacts cause cloudiness changes and due to this effect, an RF change should be multiplied by a factor of 4.2. By applying this factor, the temperature impact of the TSI change of 1.1 Wm^{-2} from 1750 to 2020 would be 0.32 °C.

3.9 Tree-ring analyses covering the last millennium

Climatic variations leave their mark on the annual rings of trees making it possible to study climate variations. Their thickness growth (tree-ring width) is controlled by the average summer temperature in cool areas and precipitation in arid regions. With the development of dendrochronological methods and the global expansion of research data, the time perspective of research covers the Holocene climate retrospectively. The tree rings are in a special position, as they are the only representative of the year-accurate proxies. In Fig. 10 the results of four tree-ring analyses have been depicted.

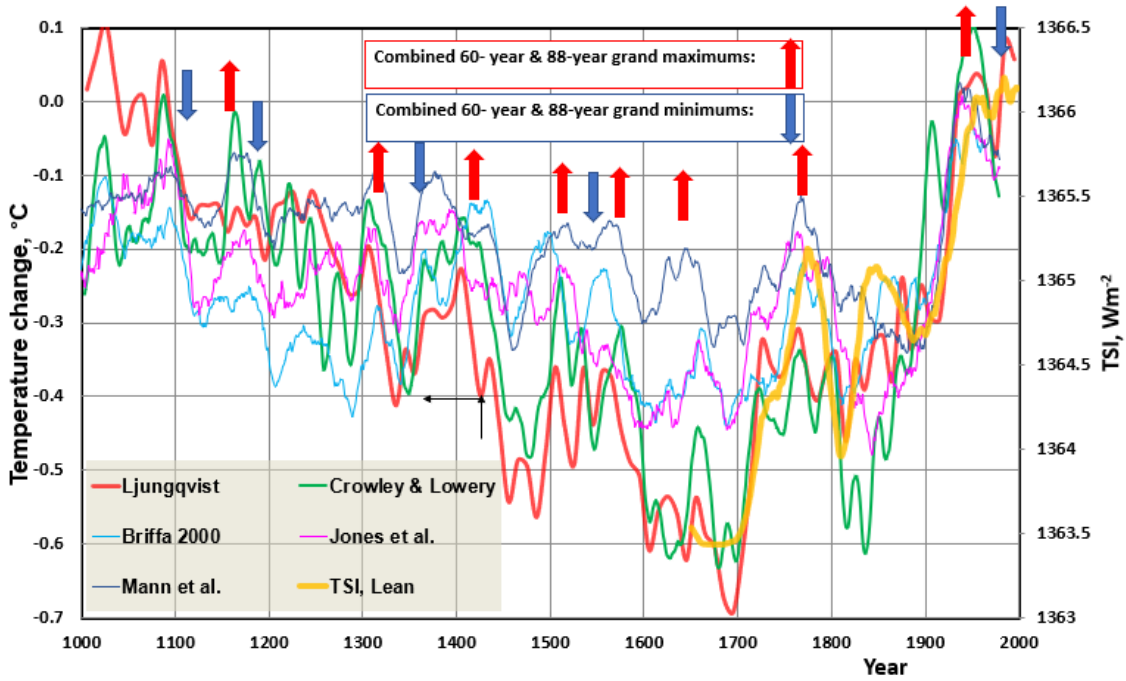

Figure 10: The proxy temperature results of Ljungqvist (2010) and the tree-ring analyses of Crowley and Lowery (2000), Briffa (2000), Jones et al. (1998), and Mann et al. (1999). The grand maximums and minimums of 60- and 88-year oscillations have been marked (Ollila and Timonen, 2022).

There are differences in the trends of different tree-ring analyses. Anyway, there is a common tendency that temperatures to start to decline after the beginning of the millennium, there is a minimum during the LIA in the 15th century, and the temperature starts to increase thereafter.

3.10 Summary of temperature proxies of the last millennium

In Fig. 11 three different types of temperature-related proxies have been depicted.

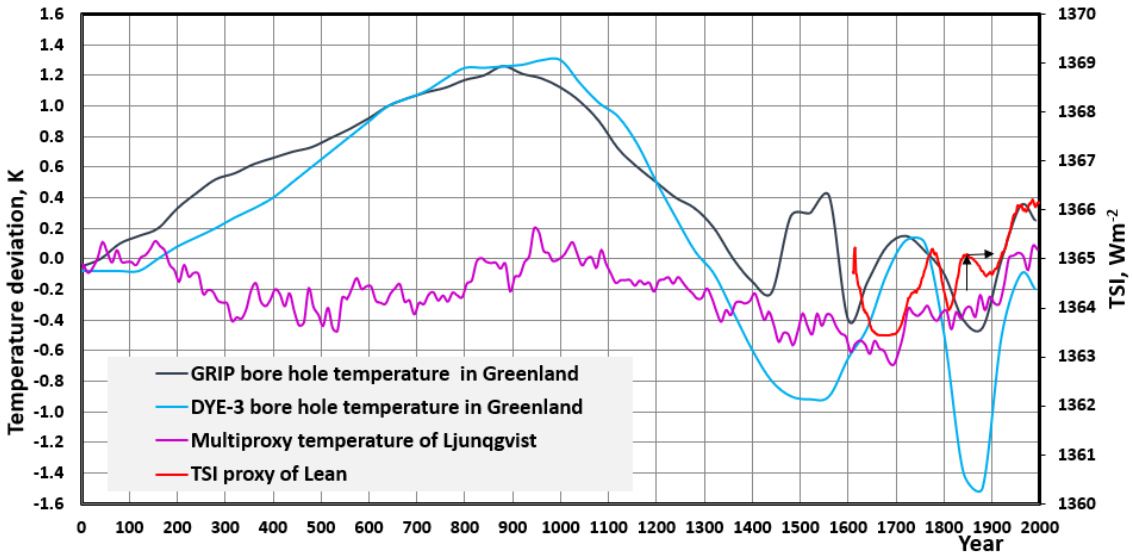

Figure 11: Two proxy temperatures of Greenland's borehole data (Vinther et al, 2011), the multiproxy temperature proxy of Ljungqvist (2010), and the TSI proxy of Lean (1995).

Borehole temperature proxies smooth out short-term variations but they indicate a period of about 1000 years having maximum peaks in about 1000 and the present maximum in 2000 (Hughes et al., 2020; Vinther et al., 2010). The temperature variations seem to be much greater in Greenland than globally, which has also been noticed during the last 50 years.

The temperature data of Ljungqvist (2010) include nine types of temperature data, namely two historical documentary records, three marine sediment records, five lake sediment records, three speleothems $\delta^{18}O$ records, two ice-core $\delta^{18}O$ records, four varved thickness sediment records, five tree-ring width records, five tree-ring maximum latewood density records, and one $\delta^{13}C$ tree-ring record. Because of the combination of different trends, this proxy is rather heavily averaged.

All these proxies show the same kind of temperature trend that during the last millennium, there have been about 1000 yearlong climate oscillations, which are caused by solar activity variations. The Earth is recovering from the LIA and is now at a new maximum.

The IPCC has concluded that the present high temperatures of the 2000s are unprecedented (IPCC, 2013). If the scrutiny period is 2000 years backward, we need not rely on temperature proxy methods only, which show two warm periods (Ljungqvist, 2010) namely the Roman warm period from 250 BC to AD 450 and the Middle Ages warm period from AD 950 to 1250. These well-known warm periods have not happened only in Europe and in North America. Li et al. (2023) have found that during the last 3500 years, the maximum precipitation and temperatures from May to October occurred on the northeastern Tibetan Plateau during the period of 800 – 1400 rather than during the current warm period.

There is also concrete evidence of warmer periods other than temperature proxies. The Lendbreen glacier in Norway is melting and it revealed a well-preserved fabric, which was made, according to radiocarbon dating, between AD 230 to 390 (Vedeler and Jorgensen, 2013). Retreating Mendenhall glaciers in Alaska has exposed forest remnants growing from 700 to 1000 based on the radiocarbon method according to the statement of Professor Connor (2013). These examples show that these warm periods have been long and at least as warm as the present ones.

3.11 Shortwave radiation anomaly of the 2000s

A significant shortwave (SW) radiation anomaly (later SW_{net}) has been observed by the CERES (2021) satellite measurements from 2001 onward. This trend has been depicted in Fig. 2(a) of Loeb et al. (2021) and in Fig. 7.3 of AR6 (IPCC, 2021). Loeb et al. (2021) concluded that the SW anomaly is probably due to the changes in low-level clouds, and the reasons for these changes may be natural and not known by climate researchers. The SW_{net}, varies according to yearly values of CERES (2021) from 240.36 Wm^{-2} in 2001 to 241.97 Wm^{-2} in 2019, which means an increase of 1.61 Wm^{-2}.

The significant SW anomaly of the 2000s (depicted as shortwave radiation downwelling in Fig. 12) is a reality but its warming impact has not been generally acknowledged in climate science since it challenges the basis of GCMs.

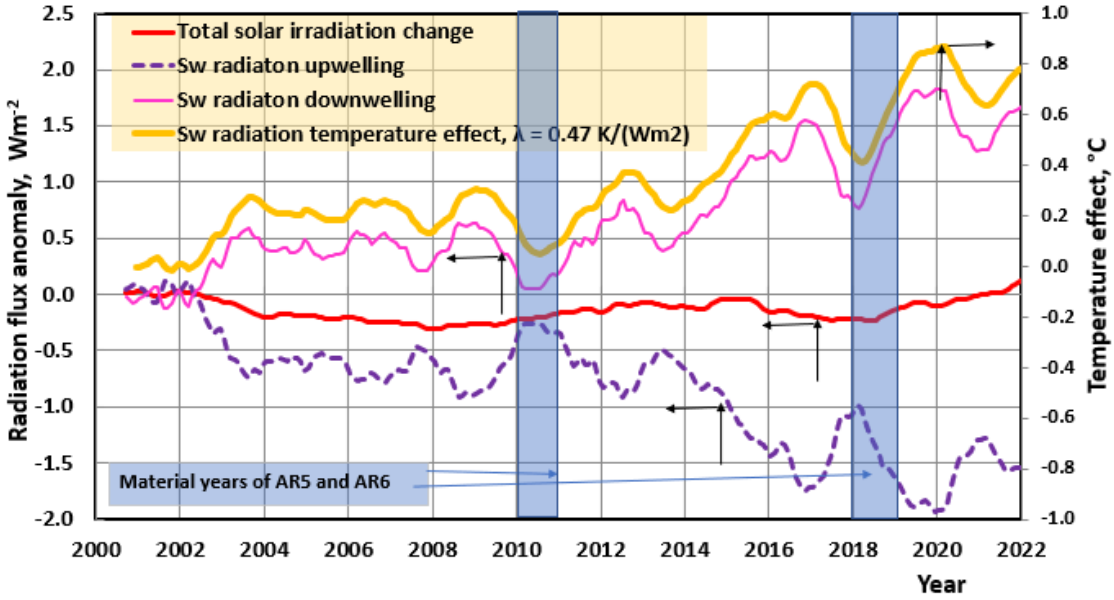

Figure 12: SW and LW radiation changes at the TOA from 2001 to 2020 (Ollila, 2021). The SW_{net} change is the same as the Shortwave radiation downwelling.

The most important issues in climate change are the RF value of CO_2 and the positive water feedback. The SW radiation anomaly of the 2000s created a unique opportunity to test the accuracies of the GCMs applied by the IPCC and a challenging model of Ollila (2021). According to the glossary of AR5 (IPCC, 2013), the portion of any top-of-atmosphere radiative effect that is due to anthropogenic or other external influences, such as changes in the Sun, is termed instantaneous radiative forcing (IRF).

Ollila (2021) simulated the temperature effects during SW radiation anomaly from 2001 to 2019 using both the IPCC's simple climate model and his simple climate model by starting temperature changes from zero in 2001, Fig. 13. In the IPCC model, a λ value of 0.47 Wm^{-2} was applied, and the CO_2 impact was calculated using Eq. (1) and (2), but the other GH gas effects were omitted due to their insignificant impact in the 20-year simulation period. Also, long-term (from 60 to 1000 years) temperature oscillations effects were omitted. For this study, the earlier simulations of the Ollila model were repeated using Eq. (2), with the λ value of 0.265 Wm^{-2}, and the RF value of CO_2 was calculated using Eq. (1). The temperature impact dT of the ENSO effect has been calculated from the Oceanic Nino Index (ONI, 2021), dT = 0.1 * ONI with 6 months delay (Trenberth and Fasullo, 2013; Ollila (2021). The dynamical time constants for the ocean were 2.74 months, and for land, 1.04 months (Stine et al., 2009).

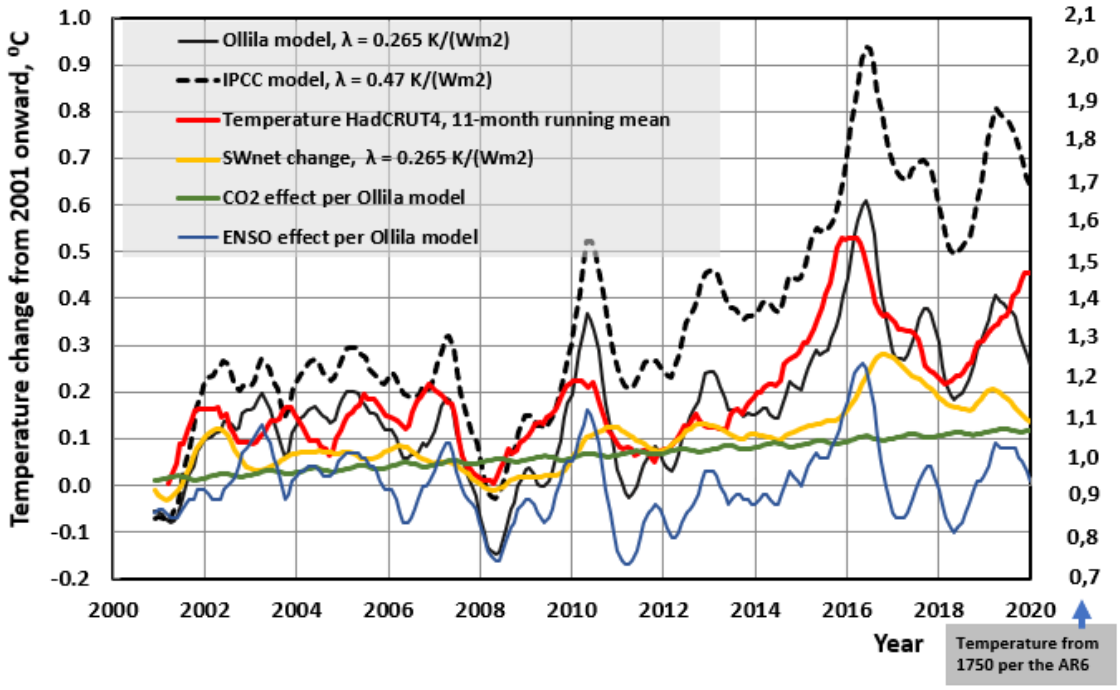

Figure 13: Calculated and observed temperature changes from 2001 to 2020. The SW_{net} changes are the same as in Fig. 11 caption.

The SW_{net} anomaly with the magnitude of 1.75 Wm^{-2} took place under real climate conditions from January 2001 to December 2021; the observed HadCRUT4 (2021) temperature change was 0.46 °C.

The temperature change from 2001 to 2019 according to the IPCC model (Ollila, 2021) is the sum of the SW_{net} change, 0.78 °C, anthropogenic drivers, 0.30 °C, and the ENSO effect, 0.03 °C, to give a total of 1.11 °C, meaning a deviation of +0.65 °C in respect to HadCRUT4 temperature. The Ollila model (Ollila, 2021) is the sum of a SW_{net} change of 0.40 °C, CO_2 forcing of 0.10 °C, an ENSO effect of 0.03 °C, and cloud effects of -0.01 °C, for a total of 0.52 °C, meaning a deviation of +0.06°C in respect to HadCRUT4.

Both model-calculated temperatures follow the ups and downs of the global observations very well indicating that the dynamical time constants are correct. The temperature errors of the IPCC's model are due to the positive water feedback and strong RF value of CO_2.

It is also interesting to note that during the period from 1979 to 2016, the average error of 102 CMIP5 test runs by Christy (2017) to the observed temperature was 0.55 °C, which is close to the temperature impact of the SW anomaly of 0.43 °C as calculated by Ollila (2021) from 2001 to 2019 applying simple models.

The IPCC dropped out this change in AR6 model-based temperature calculations since the solar impact has been -0.01°C. If the real change according to the IPCC science would have been used, the model-calculated temperature change would have been the IPCC-reported temperature increase of 1.27 °C plus the temperature effect of SW anomaly 0.76 °C totaling 2.03 °C and thus exceeding the Paris agreed temperature limit.

3.12 The summary of anthropogenic and natural drivers

The magnitudes of climate drivers have been summarized in Table 4.

Table 4. The main anthropogenic and natural drivers of surface temperature changes according to IPCC (2013), IPCC (2021), and this study named NAGW from 1750 to 2019. The values in parentheses are calculated according to the IPCC science if the SW anomaly of the 2000s is included.

Driver	IPCC/AR5 °C	IPCC/AR6 °C	NAGW/this study °C
Carbon dioxide	0.84	1.01	0.36
Methane	0.49	0.28	0.14
Nitrogen oxide	0.09	0.10	0.04
Other anthropogenic gases	0.18	0.44	-
Greenhouse gases	1.59	1.83	0.54
Albedo, volcanic	-0.08	-0.09	-
Aerosols, clouds, and contrails	-0.42	-0.49	-
Anthropogenic totally	1.11	1.28	0.54
Solar	0.03	-0.01	0.32
SW radiation anomaly	-	0.00 (0.78)	0.43
Drivers totally	1.17	1.27 (2.03)	1.29
Observed temperature change	0.85	1.29	1.29
Deviation	+37.7%	-1.6% (57%)	0.0%

The most essential result is that according to AR6 (IPCC, 2021), the contribution of CO_2 during the industrial era has been 1.01 °C but according to this study it is 0.36 °C and according to Harde (2022) it is 0.34 °C.

The trend in climate driver magnitudes from AR5 to AR6 is consistent. The most striking feature is the temperature deviation percentage change from +37.7% in 2011 to -1.6% in 2019 (material years of AR5 and AR6). This change cannot be explained by the abrupt increase of anthropogenic drivers as noticed in Table 4. A possible reason could be that the surface temperature has paused as it did in the period from 2000 to 2014 but the temperature increase rate has been greater than normal since 2014. The most probable reason is the emerging SW radiation anomaly resulting in +0.43 °C from 2001 to 2019 as indicated in the last column.

3.13 The GH effect and contribution of GH gases

The temperature effect of the GH effect is generally accepted to be 33-34 °C but the radiative forcing on the Earth's surface causing this temperature increase is getting almost no attention. The cause of the GH effect can be found only in GH effect definitions. The first comprehensive scientific definition of the GH effect based on the present-day knowledge of radiation fluxes and the effects of clouds has been presented by Hartmann (2015): *"Most of this emitted infrared radiation is absorbed by trace gases and clouds in the overlying atmosphere. The atmosphere also emits radiation, primarily at infrared wavelengths, in all directions. Radiation emitted downward from the atmosphere adds to the warming of Earth's surface by sunlight. This enhanced warming is termed the greenhouse effect.*"

This has not been good enough for the IPCC, which introduced its own definition in the AR5 (2013): *"The longwave radiation (LWR, also referred to as infrared radiation) emitted from the Earth's surface is largely absorbed by certain atmospheric constituents - (greenhouse gases and clouds) - which themselves emit LWR into all directions. The downward directed component of this LWR adds heat to the lower layers of the atmosphere and to the Earth's surface (greenhouse effect)."*

They may look very similar, but there is a crucial difference. The AR5 defines that only GH gases and clouds are responsible for the GH effect. Hartmann does not detail the components of the atmosphere causing LW radiation downwards but it is the atmosphere itself, which causes the infrared radiation. So, there might be other energy sources that warm up the atmosphere as solar radiation is absorbed by the atmosphere. It should be noticed that the term "reradiation by the atmosphere" is incorrect since if a photon has been absorbed, it does not exist anymore, and the atmospheric molecules emit new photons according to Planck's law that any material, which has a temperature above absolute zero, will emit electromagnetic radiation according to its temperature.

Ollila (2019) introduced his definition in 2019 and it considers all the energy fluxes warming the atmosphere: *"The Earth's surface emits LW radiation (infrared radiation) and it transfers heat energy in the form of latent and sensible heating into the atmosphere. Most of the emitted infrared radiation is absorbed by trace gases and clouds in the atmosphere. All three energy fluxes increase the temperature of the atmosphere. The part of the infrared radiation due to these three energy sources emitted downward from the atmosphere adds to the warming of Earth's surface by sunlight and it is called the greenhouse effect."*

In AR6 the IPCC (2021) reformulated the GH effect definition and it can be found only in the Glossary:

"The infrared radiative effect of all infrared-absorbing constituents in the atmosphere. Greenhouse gases (GHGs), clouds, and some aerosols absorb terrestrial radiation emitted by the Earth's surface and elsewhere in the atmosphere. These substances emit infrared radiation in all directions, but, equal, the net quantity emitted to space is normally less than would have been emitted in the absence of these absorbers because of the decline of temperature with altitude in the troposphere and the consequent weakening of emission. An increase in the concentration of GHGs increases the magnitude of this effect; the difference is sometimes called the enhanced greenhouse effect."

This definition does not specify anymore that only the GH gases and clouds are responsible for the downward LW radiation to the Earth's surface like in the AR5 since this radiation has not been noticed: only radiation to all directions but the radiation to the surface has not been considered at all. It can be speculated that the IPCC noticed its issue in the AR5 definition that the absorption of LW radiation of about 155 Wm^{-2} cannot create radiation of about 345 Wm^{-2} and tried to fix the problem. This time the IPCC does not show what is causing the GH effect by omitting the downward radiation which is the essence of the GH effect. If you remove the downward radiation, you remove the GH effect.

The existence of the GH effect is a generally acknowledged fact among researchers but the magnitude (the numerical value) of radiative drivers causing the GH effect has not been analyzed in the assessment reports of the IPCC. The GH effect can be illustrated by the energy budget of the Earth, Fig. 14.

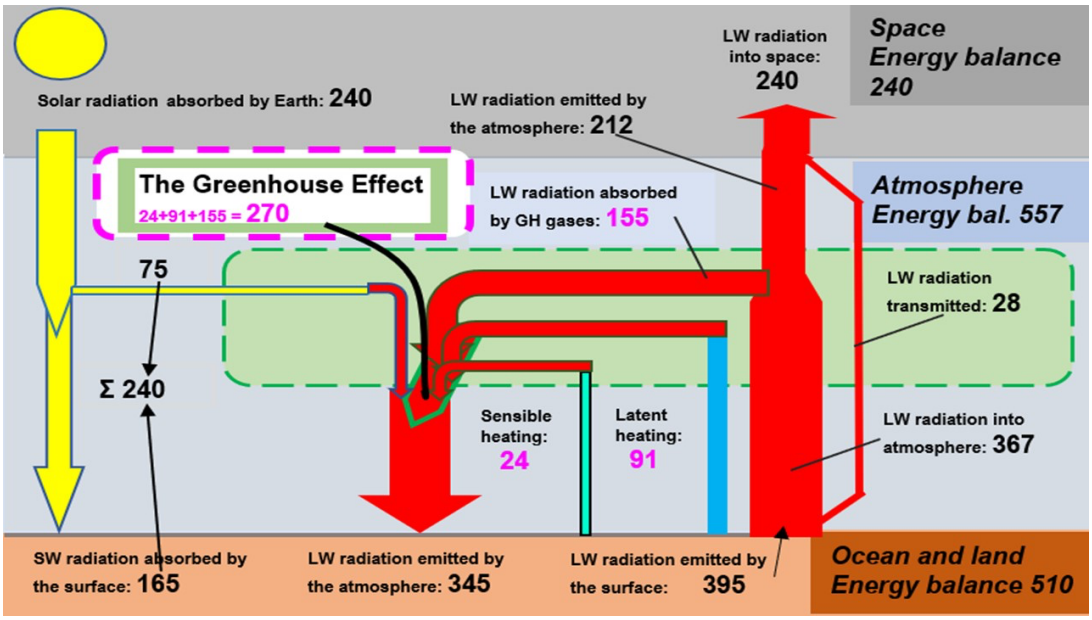

Figure 14: The Earth's energy balance (Ollila, 2019).

The presentation in Fig. 14 is from Ollila (2019), and its numerical flux values are inside the uncertainty limits of Wild et al. (2019), which has been referred to in the AR6 (IPCC, 2021).

The magnitude of the GH effect can be summarized from the flux values in Fig. 9. The downward LW flux of 345 Wm^{-2} to the surface is a sum of four fluxes (Wm^{-2}): the absorption of SW radiation 75, LW absorption by GH gases and clouds 155, latent heating 91, and sensible heating 24. The SW absorption flux of 75 Wm^{-2} together with the SW flux to the surface of 165 Wm^{-2} encompasses the net SW radiation of 240 Wm^{-2} to the Earth. The conclusion is that the "extra" radiation to the surface is the sum of three energy fluxes recirculating between the surface and the atmosphere, and its magnitude is 270 Wm^{-2} (345-75 = 270).

We have now two radiation fluxes showing the magnitude of the GH effect: the LW absorption of 155 Wm^{-2} and the additional LW radiation of 270 Wm^{-2} to the surface. Let us call them the GH effect (GHE) and the total GH effect (TGHE) respectively. Both key figures are facts and they unveil different qualities about the GH phenomenon.

There is an ongoing debate in social media about the existence of the GH phenomenon and whether it exists or not. GH effect deniers either say that the downward LW radiation flux of 345 Wm^{-2} is not real or it cannot warm the surface, since it radiates from the atmosphere being colder that the surface. This flux is real and its value can be confirmed by the worldwide measurement network (Driemel et al, 2018). Another piece of evidence about its reality and meaning is the fact since the energy budget of the surface cannot be closed without this radiation flux. The rate of radiation heat transfer from a body at temperature T_1 which is surrounded by a body at temperature T_2 is given by the Stefan-Boltzmann law

$$Q = \sigma A \varepsilon (T_1^4 - T_2^4)\ [Wm^{-2}], \qquad (7)$$

where σ is the Stefan–Boltzmann constant, A is the surface area of the radiator, and ε is the emissivity. The equation means that there is also a heat transfer rate from a colder body since all material radiates electromagnetic radiation according to Planck's law. The surface temperature T_1 is a result of these two heat transfer rates. The observation based on average radiation flux values over the period 1985-1988 shows that in the clear-sky conditions, the LW radiation upward is 394.1 Wm^{-2} and downward 313.5 Wm^{-2} but in the cloudy-sky conditions LW radiation upward

is 396.3 $Wm^{-2,}$ and downward 359.0 Wm^{-2}. These figures mean that during relatively short periods of a few days (about two days of three are cloudy), the surface temperature is higher in cloudy-sky conditions even though the SW radiation to the surface decreases by 68.3 Wm^{-2}. This would not be possible without the simultaneous increase of LW radiation by 45.5 Wm^{-2}.

Practical examples of the warming effect of different sky conditions and the S-B law are carports used in Scandinavian countries: the car windows below open car roofs stay clear in temperatures from -0 °C to -25 °C when adjacent car windows under the open sky become frozen.

LW absorption by GH gases and clouds 155 Wm^{-2} has been the basis for calculating the contributions of GH gases and clouds to the GH effect. The most referred figure (Kiehl and Trenberth, 2009) of the CO_2 contribution is 26 %. Climate change researchers should realize that this result is calculated in the modified US Standard Atmosphere 76 (US 76) containing 50 % less water than the average global atmosphere (Ollila, 2014). The US 76 has also been called "a standard atmosphere", creating a wrong image (Liou, 1992).

Schmidt et al. (2010) have used the average atmospheric composition and the GH effect magnitude of 155 Wm^{-2} in calculating the contributions of GH gases and clouds in the GH effect. Their results and the same of Ollila (2017a) have been summarized in Table 5.

Table 5. The contributions of GH gases and clouds in the GH effect according to Kiehl & Trenberth (1997), Michell (1989), Schmidt et al. (2010), and Ollila (2017a). Kiehl & Trenberth percentages in parentheses are for cloudy sky conditions.

GH effect element, RF	Ollila		Kiehl & Trenberth	Michell	Schmidt et al.
	Wm^{-2}	*%*	*%*	*%*	*%*
Water	90.9	33.6	60 (38)	65	50
Carbon dioxide	20.1	7.4	26	32	19
Ozone	6.9	2.6	8	1	
Methane & Nitrogen oxide	1.8	0.7	6	2	7
Clouds	35.9	13.3	(39)		25
LW absorption	155.6		125 (155)		155
Latent heating	90.8	33.6			-
Sensible heating	24.2	8.9			-
GH effect	270.6		155		155

Michell (1989) has not specified the atmosphere. Schmidt et al. (2010) have used a different calculation basis not used by any other researcher for CO_2 contribution by using an average value of two conditions: removing CO_2 from the average atmosphere and CO_2 being the only GH gas in the atmosphere.

The major reason for a much lower contribution-% of CO_2 by Ollila (2017a) is the magnitude of the GH effect 270.6 Wm^{-2} versus the 155 Wm^{-2} of Schmidt et al. (2010); the absorption value of CO_2 is practically the same in both papers. A counterargument against the calculation basis of 270 Wm^{-2} could be that latent heating does not change the surface temperature, and the difference between the surface emitted radiation 395 Wm^{-2} and the net radiative flux from the Sun is 395 – 240 = 155 Wm^{-2}, which is exactly the absorption magnitude by GH gases and clouds.

There is another issue and it is the contribution of GH gases to the GH effect and especially that of CO_2. The downward LW flux of 345 Wm^{-2} is the sum of all four energy fluxes warming the atmosphere. This radiation flux warms up the surface even-handed on the global scale. We cannot conclude that the latent heating energy originates only from the latent heating part of atmospheric

LW radiation. In the same way, we cannot conclude that the SW absorption flux of 75 Wm^{-2} contributes only to the radiation capability of the surface, but it does not contribute the latent and sensible heating. Every component warming up the atmosphere contributes to the TGHE according to its energy flux absorbed in the atmosphere. The situation in the climate zones shows that latent and sensible heating is mainly related to the high temperatures of the tropical zone.

Those researchers who want to show how important the role of CO_2 has in climate change prefer to use the GHE definition since it gives a much higher contribution-% in the GH effect than the TGHE definition: 26 or 19 % versus 7.4 %. The latter key figure is according to physical laws.

5. Conclusions and discussion

The alternative climate model NAGW including natural and anthropogenic drivers can explain the long-term global warming from 1750 onward as well the short-term warming during the 2000s.

The summary of the differences between the most important key figures of the IPCC model and the challenging NAGW is tabulated in Table 4. The known TSI variations have an important role in explaining the warming before 1880. There are two warming periods since 1930 and the cycling AHR effects can explain these periods of 60-year intervals. The warming mechanisms of TSI and AHR include cloudiness changes and these quantitative effects are based on empirical temperature changes. This review concludes that the NAGW has a solid theoretical background, and its warming value has better conformity with the observed temperature than the AGW. The major parameters of the AR6 (IPCC, 2021) and the parameters applied in the NAGW are collected in Table 6.

Table 6. The summary of differences between the IPCC (2021) and this study including uncertainty limits.

Parameter	AR6, IPCC	NAGW
CO_2 contribution to the GH effect	19 % – 26 %	7 % – 8 %
H_2O contribution in the GH effect	50 % – 69 %	66 % – 69 %
Water feedback	Amplifies GH gas effects by a factor from 2 to 3	Only short-term (1-2 years) positive feedback
Climate sensitivity parameter (λ)	0.47 K/(Wm^{-2}) ± 0.03	0.265 K/(Wm^{-2}) ± 0.05
RF value of 2xCO_2	3.93 Wm^{-2} ± 0.47 Wm^{-2}	2.4 Wm^{-2} ± 0.3 Wm^{-2}
Anthrop. CO_2 in the atmosphere in 2019	265 GtC	70 GtC ± 3 GtC
The residence time of anthropogenic CO_2	From centuries to millennia	16 years ± 1 years
The residence time of total CO_2	Same as anthropogenic CO_2	70 years ± 10 years
Transient Climate Response – TRC	1.8 ºC (1.4 ºC + 2.2 ºC)	0.6 ºC ± 0.1ºC
Equilibrium climate sensitivity - ECS	3.0 ºC (2.5 ºC – 4.0 ºC)	0.6 ºC ± 0.1 ºC
Greenhouse effect	159 Wm^{-2}	270 Wm^{-2}

The differences and the reason for them are already clarified in the former sections. The most important differences are the water feedback and the RF formula of CO_2. These two differences explain the differences in CS values. Considering the future atmospheric CO_2 concentration development trend, also the residence time difference is very essential. Table 6 does not show the temperature effect of the SW radiation anomaly, which is not included in GCM simulations in the AR6 calculations for 2019, and which is about 0.78 °C.

Because the Sun's activity should be decreasing and the AHR effect also declines after a few years, the global temperature according to this alternative warming theory should decline permanently after 2020 even though the warming effect of GH gases increases steadily.

Conflicts of interest/competing interests: The author has no conflicts of interest to declare that are relevant to the content of this article.

Funding: No funding was received for conducting this study.

Guest-Editor: Stein Bergsmark; Reviewers: anonymous.

References

Agnihotri R, Dutta K, Bhushan R, Somayajulu BLK, 2002: *Evidence for solar forcing on the Indian monsoon during the last millennium*. Earth and Planet Sci Lett, 198, 521-527. https://doi.org/10.1016/S0012-821X(02)00530-7

Attolini MR, Cecchini S, Galli M, Nanni T, 1987: *The Gleissberg and 130-year periodicity in the cosmogenic isotopes in the past: The Sun as a quasi-periodic system.* Proceedings of the 20th International Cosmic Ray Conference, Moscow, 4, 323, Nauka, Moscow. https://articles.adsabs.harvard.edu/pdf/1987ICRC...20d.323A

Bard E, Raisbeck G, Françoise You F, Jouzel J, 2000: *Solar irradiance during the last 1200 years based on cosmogenic nuclides.* Tellus, 52B, 985–992. https://doi.org/10.1034/j.1600-0889.2000.d01-7.x

Barrett J, Bellamy D, Hug H, 2006: *On the sensitivity of the atmosphere to the doubling of the carbon dioxide concentration and on water vapour feedback.* E&E, 17(4), 603-607. https://sci-hub.wf/10.1260/095830506778644198

Bengtsson L, Schwartz SE, 2013: *Determination of a lower bound on Earth's climate sensitivity.* Tellus B Chem Phys Meteorol, 65:1. DOI: 10.3402/tellusb.v65i0.21533

Berry EX, 2021*: The impact of human CO_2 of atmospheric CO_2.* Sci Clim Change, 1.2, 213-249. https://scienceofclimatechange.org/wp-content/uploads/Berry-2021-Impact-of-human-CO2.pdf

Briffa KR, Osborn TJ, Schweingruber FH, Harris IC, Jones PD, Shiyatov SG, Vaganov EA, 2001: *Low-frequency temperature variations from a northern tree ring density network.* J Geophys Res Atmos, 106, 2929–2941. https://doi.org/10.1029/2000JD900617

Bond G, 1997: *A Pervasive Millennial-Scale Cycle in North Atlantic Holocene and Glacial Climates*. Science, 278(5341), 1257–1266. DOI: 10.1126/science.278.5341.1257

CERES, 2021: The National Oceanic and Atmospheric Administration (NOAA), *CERES EBAF-TOA Data*: https://ceres-tool.larc.nasa.gov/ord-tool/jsp/EBAFTOA41Selection.jsp

Chen D, Wang H, Sun J, Gao Ya, 2018: *Pacific multi-decadal oscillation modulates the effect of Arctic oscillation and El Niño southern oscillation on the East Asian winter monsoon*. Int J Clim, 38, 2808-2818. https://doi.org/10.1002/joc.5461

Christy JA, 2017: *Testimony. U.S. House Committee on Science, Space & Technology*. https://docs.house.gov.pdf

Cini Castagnoli G, Bonino G, Serio M, Sonett CP, 1992: *Common spectral features in the 5500-year record of total carbonate in sea sediments and radiocarbon in tree rings*. Radiocarbon, 34(3), 798–805. DOI: https://doi.org/10.1017/S0033822200064109

Connolly R, Soon W, Connolly M, Baliunas S, Berglund, 2021: *How much has the Sun influenced Northern Hemisphere temperature trends? An ongoing debate* . Res Astron Astrophys, 21, 31. https://iopscience.iop.org/article/10.1088/1674-4527/21/6/131/meta

Connor C, 2013: *Statement of Professor Connor.* Ancient forest thaws from melting glacial tomb. https://www.livescience.com/39819-ancient-forest-thaws.html

Crowley TJ, Lowery TS, 2000: *How Warm Was the Medieval Warm Period?* J Hum Environ Stud, 29(1), 51–54. https://doi.org/10.1579/0044-7447-29.1.51

Dansgaard W, Johnsen SJ, Clausen HB, Dahl-Jensen D, Gundestrup N, Hammer CU, Oeschger H, 1984: *North Atlantic climatic oscillations revealed by deep Greenland ice cores.* Geophys Monogr Ser Climate Processes and Climate Sensitivity 29, 288–298. https://doi.org/10.1029/GM029p0288

Dansgaard W, Johnsen SJ, Clausen HB, Dahl-Jensen D, Gundestrup NS, Hammer CU, Hvidberg CS, Steffensen JP, Sveinbjörnsdottir AE, Jouzel J, 1993: *Evidence for general instability of past climate from a 250-kyr ice-core record*. Nature, 364(6434), 218–220. https://doi.org/10.1038/364218a0

Davis WJ, 2017: *The relationship between atmospheric carbon dioxide concentration and global temperature for the last 425 million years*. Climate *5*(4), 76. https://doi.org/10.3390/cli5040076

Davis W, Taylor P, Davis W, 2018: *The Antarctic centennial oscillation: A natural paleoclimate cycle in the southern hemisphere that influences global temperature.* Climate, 6(1), 3. https://doi.org/10.3390/cli6010003

Davis WJ, Taylor PJ, Davis WB, 2019: *The origin and propagation of the Antarctic centennial oscillation. Climate*, 7(9), 112. https://doi.org/10.3390/cli7090112

Driemel A, Augustine J, Behrens K, Colle S, Cox C, et. 2018: *Baseline Surface Radiation Network (BSRN): structure and data description (1992–2017)*. Earth Sys Sci Data, 10(3), 1491-1501. https://doi.org/10.5194/essd-10-1491-2018

Drotos G, Becker T, Mauritsen T, Stevens B, 2020: Global variability in radiative-convective equilibrium with a slab ocean under a wide range of CO_2 concentrations. Tellus A: Dyn Meteorol Oceanogr, 72(1), 1–1. https://sci-hub.wf/10.1080/16000870.2019.1699387

Ermakov VJ, Okhlopkov VP, Stozhkov YuI, 2009: *Influence of cosmic rays and cosmic dust on the atmosphere and Earth's climate*. Bull Russ Acad Sci: Phys, 73, 434-436. https://doi.org/10.3103/S1062873809030411

Etminan E, Myhre G, Highwood EJ, Shine KP, 2016: *Radiative forcing of carbon dioxide, methane, and nitrous oxide: A significant revision of methane radiative forcing*. Geophys Res Lett 43:12614-12636. https://doi.org/10.1002/2016GL071930

Feynman J, Fougere PF, 1984: *Eighty-eight-year periodicity in solar-terrestrial phenomena confirmed*. J Geophys Res: Space Phys, 89, 3023–3027. https://doi.org/10.1029/JA089iA05p03023

Fleming RJ, 2018: *An updated review about carbon dioxide and climate change.* Environ Earth Sci, 77(6), 262–. https://link.springer.com/article/10.1007/s12665-018-7438-y

Folland CK, Parker DE, Kates FE, 1984: *Worldwide marine temperature fluctuations 1856–1981*. Nature, 310, 670–673. https://doi.org/10.1038/310670a0

Folland CK, Parker DE, Kates FE, 1986: *Sahel rainfall and worldwide sea temperatures, 1901-85.* Nature, 320, 602-607. https://doi.org/10.1038/320602a0

Friedlingstein P, Jones MW, O'Sullivan M, Robbie MA, Hauck J, et al., 2020: *Global Carbon Budget 2020.* Earth Syst Sci Data 12:3269-3340. https://doi.org/10.5194/essd-12-3269-2020

Gats, 2014: *Spectral calculations tool*, http://www.spectralcalc.com/info/about.php

Gervais F, 2021: *Climate sensitivity and carbon footprint.* Sc Clim Change, 1.1, 70-97. https://scienceofclimatechange.org/wp-content/uploads/Gervais-2021-Climate-Sensitivity-Carbon-Footprints.pdf

Gruber N, Clement D, Carter B, Feely RA, van Heuven S, Hoppema M, Ishii M, Key RM, Kozyr A, Lauvset SK, Lo Monaco C, Mathis JT, Murata A, Olsen A, Perez FF, Sabine, CL, Tanhua T, Wanninkhof R, 2019: *The oceanic sink for anthropogenic CO_2 from 1994 to 2007.* Science, 363(6432), 1193–1199. doi: 10.1126/science.aau5153

Hale GE, 1908: *On the probable existence of a magnetic field in sunspots*. Astrophys J, 28, 315-343. 10.1086/141602

HadCRUT4, 2021: *HaDCRUT4 temperature data of Met Office Hadley Centre.* https://www.metoffice.gov.uk/hadobs/hadcrut4/

Harde H, 2013: *Radiation and heat transfer in the atmosphere: A comprehensive approach on a molecular basis.* Int J Atmos Sci, ID 503727. https://doi.org/10.1155/2013/503727

Harde H, 2017: *Radiation transfer calculations and assessment of global warming by CO2*. Int J Atmos Sci, https://downloads.hindawi.com/archive/2017/9251034.pdf

Harde H, 2022: *How Much CO2 and the Sun Contribute to Global Warming: Comparison of Simulated Temperature Trends with Last Century Observations.* Sc Clim Change, 2.2, 105-133. https://scienceofclimatechange.org/wp-content/uploads/Harde-2022-CO2-Sun-Global-Warming.pdf

Harde H, Salby ML, 2021: *What Controls the Atmospheric CO2 Level?* Sci Clim Change, 1.1, 54-69. https://scienceofclimatechange.org/wp-content/uploads/Harde-and-Salby-2021-What-Controls-CO2.pdf

Hartmann DL, 2015: *Global Physical Climatology,* Elsevier Science, USA. https://www.elsevier.com/books/global-physical-climatology/hartmann

HITRAN, 2021: *High-Resolution Transmission Molecular Absorption data base*, Harvard-Smithsonian Center for Astrophysics. https://www.cfa.harvard.edu/hitran/

Hoyt DV, Schatten KH, 1993: *A discussion of plausible solar irradiance variations, 1700-1992.* J Geophys Res, 98(A11), 18895-18906. https://doi.org/10.1029/93JA01944

Hughes AG, Jones TR, Vinther BM, Gkinis V, Stevens CM, Morris V, Vaughn BH, Holme C, Markle BR, Whiter JWC, 2020: *High-frequency climate variability in the Holocene from a coastal-dome ice core in east-central Greenland*. Clim Past, 16, 1369–1386. https://doi.org/10.5194/cp-16-1369-2020

Jones PD, Briffa KR, Barnett TP, Tett SFB, 1998: *High-resolution paleoclimatic records for the last millennium: interpretation, integration, and comparison with General Circulation Model control-run temperatures*. Holocene, 8(4), 455–471. https://doi.org/10.1191/095968398667194956

IPCC, 2001: *Climate Change 2001, The Physical Science Basis, TAR*, (eds. Salomon S. et al.). Cambridge Univ. Press, UK. https://www.ipcc.ch/site/assets/uploads/2018/03/WGI_TAR_full_report.pdf

IPCC, 2007: *Climate Change 2007, The Physical Science Basis, AR4*, (eds. Salomon S. et al.). Cambridge Univ. Press, UK. https://www.ipcc.ch/report/ar4/wg1/

IPCC, 2013: *Climate Change 2011, The Physical Science Basis, AR5*, (eds. Salomon S. et al.). Cambridge Univ. Press, UK. https://www.ipcc.ch/site/assets/uploads/2017/09/WG1AR5_Frontmatter_FINAL.pdf

IPCC, 2021: *Climate Change 2021, The Physical Science Basis, AR6*, Cambridge Univ. Press, UK. https://www.ipcc.ch/report/ar6/wg1/

Joos F, Prentice IC, Sitch S, Meyer R, Hooss G, et al., 2001: *Global warming feedbacks on terrestrial carbon uptake under the Intergovernmental Panel on Climate Change (IPCC) Emission Scenarios*, Glob Biogeochem Cycles, 15, J891-908. 10.1029/2000GB001375

Joos F. Roth R, Fuglestvedt JS, Peters GP, Enting IG, 2013: *Carbon dioxide and climate impulse response functions for the computation of greenhouse gas metrics: a multi-model analysis*. Atm Chem Phys, 13(5): 2793–2825. doi:10.5194/acp-13-2793-2013

Kauppinen J, Heinonen JT, Malmi PJ, 2014: *Influence of relative humidity and clouds on the global mean surface temperature.* E&E 25(2). https://doi.org/10.1260/0958-305X.25.2.389

Kerr RA, 2000: *A North Atlantic Climate Pacemaker for the Centuries*. Science, 288,1984-1985. DOI: 10.1126/science.288.5473.1984

Kiehl JT, Trenberth KE, 1997: *Earth's annual global mean energy budget*. Bull Amer Meteor Soc 90: 311-323. https://doi.org/10.1175/1520-0477(1997)078<0197:EAGMEB>2.0.CO;2

Kissin YV, 2015: *A simple alternative model for the estimation of the carbon dioxide effect on the Earth's energy balance*. E&E, 26(8), 1319–1333. https://doi.org/10.1260/0958-305X.26.8.1319

Klyashtorin LB, Borisov V, Lyubushin A, 2009: *Cyclic changes of climate and major commercial stocks of the Barents Sea.* Mar Biol Res, 5, 4-17. https://doi.org/10.1080/17451000802512283

Lean J, 1995: *Construction of solar irradiance since 1610: Implications for climate change*. Geophys Res Lett 22: 3195-3198. https://doi.org/10.1029/95GL03093

Lean J, 2004: *Solar Irradiance Reconstruction,* IGBP PAGES/World Data Center for Paleoclimatology Data Contribution Series # 2004-035, NOAA/NGDC Paleoclimatology Program.

Lean J, 2010: *Cycles and trends in solar irradiance.* WIREs Climate Change 1: 111-122. https://doi.org/10.1002/wcc.18

Levin I, Naegler T, Kromer B, Diehl M, Francey RJ, Gomez-Pelaez AJ, Steele LP, Wagenbach D, Weller R and Worthy DE, 2010: *Observations and modelling of the global distribution and long-term trend of atmospheric $^{14}CO_2$*. Tellus 62B, 26-46. DOI: 10.1111/j.1600-0889.2009.00446.x

Lewis N, Curry JA, 2015: *The implications for climate sensitivity of AR5 forcing and heat uptake estimates.* Clim Dyn, 45(3-4), 1009–1023. https://doi.org/10.1007/s00382-014-2342-y

Li Y, Wu D, Wang T, Chen L, Chenbin Z, 2023: *Late Holocene temperature and precipitation variations in an alpine region of the northeastern Tibetan Plateau and their response to global climate change*. Palaeogeogr Palaeoclimatol Palaeoecol 615(3), 111442. https://doi.org/10.1016/j.palaeo.2023.111442

Lin YC, Fan CY, Damon PE, Wallick EI, 1975: *Long-term modulation of cosmic-ray intensity and solar activity cycles*, 14th International Cosmic Ray Conference, Germany, Munchen, 3, 995–999. Max-Planck-Institut für extraterrestrische Physik, Germany. https://adsabs.harvard.edu/full/1975ICRC....3..995L

Liou KN, 1992: *Radiation and cloud processes in the atmosphere*. Oxford Univ. Press, UK. https://www.osti.gov/biblio/7081459

LLNL, 2016: Lawrence Livermore National Laboratory, *^{14}C "Bomb Pulse" Pulse Forensics*, https://cams.llnl.gov/cams-competencies/forensics/14c-bomb-pulse-forensics

Locean, 2016: *Oceans 13C*, https://www.locean-ipsl.upmc.fr/oceans13c/indexAng.htm

Loeb NG, Johnson GC, Thorsen TJ, Lyman JM, Rose FG, Kato S, 2021: *Satellite and ocean data reveal marked increase in Earth's heating rate*. Geophys Res Lett, 48, e2021GL093047. https://doi.org/10.1029/2021GL093047

Lungqvist FC, 2010: *A new reconstruction of temperature variability in the extra-tropical Northern Hemisphere during the last two millennia*. Geogr Ann, 92 A 3, 339–351. https://doi.org/10.1111/j.1468-0459.2010.00399.x

Manabe S, Wetherald R, 1967: *Thermal equilibrium of the atmosphere with a given distribution of relative humidity*. J Atmos Sci 24, 241–259. https://doi.org/10.1175/1520-0469(1967)024<0241:TEOTAW>2.0.CO;2

Mann ME, Bradley RS, Hughes MK, 1999: *Northern hemisphere temperatures during the past millennium: Inferences, uncertainties, and limitations.* Geophys Res Lett, 26(6), 759–762. https://doi.org/10.1029/1999GL900070

Meinshausen M, Nicholls MRJ, Lewis J, Gidden MJ, Vogel E, et al., 2020: *The shared socio-economic pathway (SSP) greenhouse gas concentrations and their extensions to 2500*. Geosci Model Dev 13, 3571–3605. https://doi.org/10.5194/gmd-13-3571-2020

Michell JFB, 1989: *The "greenhouse" effect and climate change*. Rev Geophys, 27(1), 115-139. https://doi.org/10.1029/RG027i001p00115

Miskolczi FM, Mlynczak MG, 2004: *The greenhouse effect and the spectral decomposition of the clear-sky terrestrial radiation*. Idöjaras 108, 209-251. http://owww.met.hu/idojaras/IDOJARAS_vol108_No4_01.pdf

Miskolczi FM, 2014: *The greenhouse effect and the infrared radiative structure of the Earth's atmosphere*. Dev Earth Sc 2, the greenhouse effect. https://www.researchgate.net/publication/268507883_The_Greenhouse_Effect_and_the_Infrared_Radiative_Structure_of_the_Earth's_Atmosphere

Myhre G, Highwood EJ, Shine KP, Stordal F, 1998: *New estimates of radiative forcing due to well mixed greenhouse gases*. Geophys. Res. Lett. 25, 2715-2718. https://doi.org/10.1029/98GL01908

Myhre G, Stordal F, Gausemel I, Nielsen CJ, Mathieu E, 2016: *Line-by-line calculation of thermal infrared radiation for global condition: CFC-12 as an example*. J Quant Spectros Radiat Transf 97, 317–331. https://doi.org/10.1016/j.jqsrt.2005.04.015

NOAA, 2021: *NCEP/NCAR Reanalysis Data*. https://www.esrl.noaa.gov/psd/cgi-bin/data/timeseries/timeseries1.pl

NOAA, 2018: *The data: What ^{13}C tells us, the global view 2018.* http://www.esrl.noaa.gov/gmd/outreach/isotopes/c13tellsus.html.

NOAA, 2022: *Atlantic Multidecadal Oscillation AMO (2022).* https://psl.noaa.gov/data/correlation/amon.us.long.data

NSDC, 2020: *Six tree-ring proxy data and one temperature data set.* https://www1.ncdc.noaa.gov/pub/data/paleo/tree-ring/reconstructions/n_hem_temp/briffa2001jgr3.txt

Ohmura A, 2001: *Physical basis for the temperature-based melt-index method*. J Appl Meteorol 40, 753-761. https://doi.org/10.1175/1520-0450(2001)040<0753:PBFTTB>2.0.CO;2

Ollila A, 2012: *The roles of greenhouse gases in global warming.* Energy Environ, 23(5), 781-799. https://doi.org/10.1260/0958-305X.23.5.781

Ollila A, 2013: *Dynamics between clear, cloudy and all-sky conditions: cloud forcing effects.* J Chem Biol Phys Sc 4(1), 557-575. https://www.researchgate.net/publication/274958251_Dynamics_between_clear_cloudy_and_all-sky_conditions_Cloud_forcing_effects

Ollila A, 2014: Dev Earth Sci 2, 20-30 *The potency of carbon dioxide (CO_2) as a greenhouse gas.* https://www.researchgate.net/publication/274956207_The_potency_of_carbon_dioxide_CO2_as_a_greenhouse_gas

Ollila A, 2017a: *Warming effect reanalysis of greenhouse gases and clouds*. Phys Sci Int J 13(2), 1-13. DOI: 10.9734/PSIJ/2017/30781

Ollila A, 2017b: *Semi empirical model of global warming including cosmic forces, greenhouse gases, and volcanic eruptions*. Phy Sci Int J 15(2), 1-14. DOI:10.9734/PSIJ/2017/34187

Ollila A, 2019: *The greenhouse effect definition*. Phy Sci Int J 23(2), 1-5. DOI: 10.9734/PSIJ/2019/v23i230149

Ollila A, 2020a: *The pause end and major temperature impacts during super El Niños are due to shortwave radiation anomalies*. Phys Sc Int J 24(2):1-20. DOI: 10.9734/PSIJ/2020/v24i230174

Ollila A, 2020b: *The Greenhouse effect calculations by an iteration method and the issue of stratospheric cooling*. Phy Sci Int J 24(7), 1-18. DOI: 10.9734/PSIJ/2020/v24i730199

Ollila A, 2020c: *Analysis of the simulation results of three carbon dioxide (CO_2) cycle models.* Phys Sc Int J 23(4),1-19. DOI: 10.9734/PSIJ/2019/v23i430168

Ollila A, 2021: *Global Circulations Models (GCMs) simulate the current temperature only if the shortwave radiation anomaly of 2000s has been omitted*. Phys Sc Int J 40(17), 45-52. DOI:10.9734/CJAST/2021/v40i1731433

Ollila A, Timonen M, 2022a: *Two main temperature periodicities related to planetary and solar activity oscillations*. https://hal.science/hal-04160543

ONI, 2021: *Oceanic Nino Index (ONI) of NOAA*: https://ggweather.com/enso/oni.htm

Otto A, Otto FEL, Boucher O, Church J, Hegerl G, Forster PM, Gillett NP, Gregory J, Johnson GC, Knotty R, Lewis N, Lohmann U, Marotzke J, Myhre G, Shindell D, Stevens B, Allen MR, 2013: *Energy budget constraints on climate response.* Nat Geosci, 6(6), 415–416. https://doi.org/10.1038/ngeo1836

Quay P, Sonnerup R, Westby T, Stutsman J, McNichol A, 2003: *Changes in the $^{13}C/^{12}C$ of dissolved inorganic carbon in the ocean as a tracer of anthropogenic CO_2 uptake*. Glob Biogeochem 17(1), 4-1-4-20. https://doi.org/10.1029/2001GB001817

Patterson RT, Prokoph A, Changa A, 2004: *Late Holocene sedimentary response to solar and cosmic ray activity influenced climate variability in the NE Pacific*. Sediment Geol, 172 , 67 – 84. https://doi.org/10.1016/j.sedgeo.2004.07.007

Peristykh AN, Damon PE, 2003: *Persistence of the Gleissberg 88-year solar cycle over the last ~12,000 years: Evidence from cosmogenic isotopes*. J Geophys Res: Space Phys, 108 (A1), 1003. https://doi.org/10.1029/2002JA009390

Ramanathan V, Cicerone R, Singh H, Kiehl I, 1985: *Trace gas trends and their potential role in climate change*. J Geophys Res 90, 5547-5566. https://doi.org/10.1029/JD090iD03p05547

Revelle R, Suess HE, 1957: *Carbon dioxide exchange between atmosphere and ocean and the question of an increase of atmospheric CO_2 during the past decades*. Tellus, 9(1), 18–27. https://doi.org/10.1111/j.2153-3490.1957.tb01849.x

Sabine CL, Feely RA, Gruber, Key RM, Lee K, Bullister JL, Wanninkhof R, Wong CS, Wallace DW, Tilbrook B, Millero FJ, Peng TH, Kozyr A, Ono T and Rios AF, 2004: *The oceanic sink for the anthropogenic CO_2*. Science 305, 367–371. DOI: 10.1126/science.1097403

Santer BD, Fyfe JC, Pallotta G, Flato GM, Meehl GA, England MH, Hawkins E, Mann ME, Painter JF, Bonfils C, Cvijanovic I, Mears C, Wentz GJ, Po-Chedley S, Fu Q and Zou C-Z, 2017: *Causes of differences in model and satellite tropospheric warming rates*. Nat Geosci 10, 478-485. https://doi.org/10.1038/ngeo2973

Scafetta N, 2010: *Empirical evidence for a celestial origin of the climate oscillations and its implications*. J Atmos Sol-Terr Phy 72, 951-970. https://doi.org/10.1016/j.jastp.2010.04.015

Schlesinger ME, 1986: *Equilibrium and transient climatic warming induced by increased atmospheric CO_2*. Clim Dyn, 1(1), 35–51. https://doi.org/10.1007/BF01277045

Schlesinger ME, Ramankutty N, 1994: *An oscillation in the global climate system of period 65-70 years*. Nature, 367, 723-726. https://doi.org/10.1038/367723a0

Schildknecht D, 2020: *Saturation of the infrared absorption by carbon dioxide in the atmosphere*. Int J Modern Phys B. https://arxiv.org/pdf/2004.00708.pdf

Schmidt GA, Ruedy R, Miller RL , Lacis AA, 2010: *Attribution of the present-day total greenhouse effect.* J Geophys. Res. 115, D20106. https://agupubs.onlinelibrary.wiley.com/doi/full/10.1029/2010JD014287

Schwabe SH, 1843: *Sonnenbeobachtungen im Jahre 1843 (in German).* Observations of the Sun in the year 1843. Astronomische Nachrichten 21, 233–236. 10.1002/asna.18440211505

Segalstad TV, 1998: *Carbon cycle modelling and the residence time of natural and anthropogenic atmospheric CO_2: On the construction of "greenhouse effect global warming" dogma. The continuing debate*. European Science and Environmental Forum (ESEF), Cambridge, England. 184-219. https://ww.researchgate.net/publication/237706208.pdf

Smith CJ, Kramer RJ, Myhre G et al., 2018: *Understanding rapid adjustments to diverse forcing agents.* Geophys Res Lett, 45, 2023–2031. https://doi.org/10.1029/2018GL079826

Stine AR, Huybers P, Fung IY, 2009: *Changes in the phase of annual cycle of surface temperature*. Nature, 457, 435-441. https://doi.org/10.1038/nature07675

Srivastava A, Verkouteren M, 2018: *Metrology for stable isotope reference materials: $^{13}C/^{12}C$ and $^{18}O/^{16}O$ isotope ratio value assignment of pure carbon dioxide gas samples on the Vienna PeeDee Belemnite-CO_2 scale using dual-inlet mass spectrometry*. Anal Bioanal Chem 410, 4153–4163. https://doi.org/10.1007/s00216-018-1064-0

Suess HE, 1980: *The radiocarbon record in tree rings of the last 8000 years*. Radiocarbon, 22(2), 200– 209. https://www.cambridge.org/core/journals/radiocarbon/article/radiocarbon-record-in-tree-rings-of-the-last-8000-years/EBD9056098B2151DA8027942C338F514

Trenberth KE, Fasullo JT, 2013: *An apparent hiatus in global warming*? Earth's Future, 1, 19-32. https://doi.org/10.1002/2013EF000165

UAH, 2022: *UAH MSU temperature data set of lower troposphere,* http://vortex.nsstc.uah.edu/data/msu/v6.0beta/tlt/uahncdc_lt_6.0beta5.txt

Utrecht Universiteit, 2016: *Radiocarbon dating*, http://web.science.uu.nl/AMS/radiocarbon.htm

Vedeler M, Jørgensen LB, 2013: *Out of the Norwegian glaciers: Lendbreen – a tunic from the early first millennium AD.* Antiquity 87, 788–801. https://doi.org/10.1017/S0003598X00049462

Velasco Herrera VM, Mendoza B, Velasco Herrera G, 2015: *Reconstruction and prediction of the total solar irradiance: From the Medieval Warm Period to the 21st century.* New Astron*, 34(), 221–233.* https://sci-hub.wf/10.1016/j.newast.2014.07.009

Vinther BM, Jones PD, Briffa KR, Clausen HB, Andersen KK, Dahl-Jensen D, Johnsen SJ, 2010: *Climatic signals in multiple highly resolved stable isotope records from Greenland.* Quat Sci Rev, 29(3-4), 522–538. https://doi.org/10.1016/j.quascirev.2009.11.002

Vinther BM, 2011: *The medieval climate anomaly in Greenland ice core data*. PAGES news, 19(1), 27. Vinther_2011-1_27.pdf

Wijngaarden W and Happer W, 2020: *Dependence of Earth's thermal radiation on five most abundant greenhouse gases*. https://arxiv.org/abs/2006.03098

Wild M, Hakuba MZ, Folini D, Dörig-Ott P, Schär C, Kato S, Long CN, 2019: *The cloud-free global energy balance and inferred cloud radiative effects: an assessment based on direct observations and climate models.* Clim Dyn 52, 4787–4812. https://doi.org/10.1007/s00382-018-4413-y